19. The Committee of Japan Diabetes Society on the diagnostic criteria of diabetes mellitus. Report of the Committee on the classification and diagnostic criteria of diabetes mellitus. *J Diabetes Invest* 2010; 1: 212–228.
20. Yamada Y, Fukuda K, Fujimoto S, *et al.* SUIT, secretory units of islets in transplantation: an index for therapeutic management of islet transplanted patients and its application to type 2 diabetes. *Diabetes Res Clin Pract* 2006; 74: 222–226.
21. Japan Diabetes Society. Insulin treatment. In: Japan Diabetes Society (ed.). *Treatment Guide for Diabetes 2007.* Bunkodo, Japan, 2007; 47–55.
22. Franz MJ, Monk A, Barry B, *et al.* Effectiveness of medical nutrition therapy provided by dietitians in the management of non-insulin-dependent diabetes mellitus: a randomized, controlled clinical trial. *J Am Diet Assoc* 1995; 95: 1009–1017.
23. Ziemer DC, Berkowitz KJ, Panayioto RM, *et al.* A simple meal plan emphasizing healthy food choices is as effective as an exchange-based meal plan for urban African Americans with type 2 diabetes. *Diabetes Care* 2003; 26: 1719–1724.
24. Miller CK, Edwards L, Kissling G, *et al.* Nutrition education improves metabolic outcomes among older adults with diabetes mellitus: results from a randomized controlled trial. *Prev Med* 2002; 34: 252–259.
25. Japan Diabetes Society. Diet therapy. In: Japan Diabetes Society (ed.). *Treatment Guide for Diabetes 2007.* Bunkodo, Japan, 2007; 34–37.
26. Park SW, Ihm SH, Yoo HJ, *et al.* Differential effects of ambient blood glucose level and degree of obesity on basal serum C-peptide level and the C-peptide response to glucose and glucagon in non-insulin-dependent diabetes mellitus. *Diabetes Res Clin Pract* 1997; 37: 165–171.
27. Albareda M, Rigla M, Rodríguez-Espinosa J, *et al.* Influence of exogenous insulin on C-peptide levels in subjects with type 2 diabetes. *Diabetes Res Clin Pract* 2005; 68: 202–206.
28. Peacock I, Tattersall RB. The difficult choice of treatment for poorly controlled maturity onset diabetes: tablets or insulin? *Br Med J (Clin Res Ed)* 1984; 288: 1956–1959.
29. Sakuraba H, Mizukami H, Yagihashi N, *et al.* Reduced beta-cell mass and expression of oxidative stress-related DNA damage in the islet of Japanese Type II diabetic patients. *Diabetologia* 2002; 45: 85–96.
30. Butler AE, Janson J, Bonner-Weir S, *et al.* β-cell deficit and increased β-cell apoptosis in humans with type 2 diabetes. *Diabetes* 2003; 52: 102–110.
31. Rahier J, Guiot Y, Goebbels RM, *et al.* Pancreatic β-cell mass in European subjects with type 2 diabetes. *Diabetes Obes Metab* 2008; 10: 32–42.
32. Meier JJ, Menge BA, Breuer TG, *et al.* Functional assessment of pancreatic β-cell area in humans. *Diabetes* 2009; 58: 1595–1603.

## SUPPORTING INFORMATION

Additional Supporting Information may be found in the online version of this article:

**Figure S1** | Process of selection of subjects for analysis.
**Figure S2** | Therapeutic modes of analyzed patients at admission and discharge, and the required alteration of therapy during the period of admission.
**Figure S3** | Relative frequency distribution of C-peptide indices of patients with mean preprandial capillary plasma glucose levels of <130 mg/dL at discharge in the non-insulin and insulin group.
**Table S1** | Details of medication and daily dosages of oral hypoglycemic agents used at discharge

Please note: Wiley-Blackwell are not responsible for the content or functionality of any supporting materials supplied by the authors. Any queries (other than missing material) should be directed to the corresponding author for the article.

BJ www.biochemj.org



BJ Metabolism

Biochem. J. (2011) **435**, 421–430 (Printed in Great Britain) doi:10.1042/BJ20101708



# Role of mitochondrial phosphate carrier in metabolism–secretion coupling in rat insulinoma cell line INS-1

Yuichi NISHI, Shimpei FUJIMOTO[1], Mayumi SASAKI, Eri MUKAI, Hiroki SATO, Yuichi SATO, Yumiko TAHARA, Yasuhiko NAKAMURA and Nobuya INAGAKI

Department of Diabetes and Clinical Nutrition, Graduate School of Medicine, Kyoto University, 54 Shogoin Kawahara-cho, Sakyo-ku, Kyoto 606–8507, Japan

In pancreatic $\beta$-cells, glucose-induced mitochondrial ATP production plays an important role in insulin secretion. The mitochondrial phosphate carrier PiC is a member of the SLC25 (solute carrier family 25) family and transports $P_i$ from the cytosol into the mitochondrial matrix. Since intramitochondrial $P_i$ is an essential substrate for mitochondrial ATP production by complex V (ATP synthase) and affects the activity of the respiratory chain, $P_i$ transport via PiC may be a rate-limiting step for ATP production. We evaluated the role of PiC in metabolism–secretion coupling in pancreatic $\beta$-cells using INS-1 cells manipulated to reduce PiC expression by siRNA (small interfering RNA). Consequent reduction of the PiC protein level decreased glucose (10 mM)-stimulated insulin secretion, the ATP:ADP ratio in the presence of 10 mM glucose and elevation of intracellular calcium concentration in response to 10 mM glucose without affecting the mitochondrial membrane potential ($\Delta\psi_m$) in INS-1 cells. In experiments using the mitochondrial fraction of INS-1 cells in the presence of 1 mM succinate, PiC down-regulation decreased ATP production at various $P_i$ concentrations ranging from 0.001 to 10 mM, but did not affect $\Delta\psi_m$ at 3 mM $P_i$. In conclusion, the $P_i$ supply to mitochondria via PiC plays a critical role in ATP production and metabolism–secretion coupling in INS-1 cells.

Key words: inorganic phosphate ($P_i$), insulin secretion, mitochondria, mitochondrial phosphate carrier (PiC), small interfering RNA (siRNA), solute carrier family 25 (SLC25).

## INTRODUCTION

Glucose stimulates insulin secretion by both triggering and amplifying signals in pancreatic $\beta$-cells [1]. The triggering pathway includes entry of glucose into $\beta$-cells, acceleration of glycolysis in the cytosol and mitochondrial metabolism of products derived from glycolysis, increase in ATP content and ATP/ADP ratio, closure of ATP-sensitive $K^+$ channels ($K_{ATP}$ channels), membrane depolarization, opening of VDCCs (voltage-dependent $Ca^{2+}$ channels), increase in $Ca^{2+}$ influx through VDCCs, rise in intracellular $Ca^{2+}$ concentration ($[Ca^{2+}]_i$), and exocytosis of insulin granules. Glucose also exerts its effects by increasing $Ca^{2+}$ efficacy in stimulation–secretion coupling via an amplifying pathway, owing at least in part to the direct effect of increased ATP derived from glucose metabolism on exocytosis. Since depletion of mitochondrial DNA abolishes the glucose-induced ATP elevation, mitochondria are clearly a major source of ATP production in pancreatic $\beta$-cells [2,3]. Collectively, in pancreatic $\beta$-cells, intracellular glucose metabolism regulates exocytosis of insulin granules according to metabolism–secretion coupling in which glucose-induced mitochondrial ATP production plays an important role.

Almost all of the mitochondrial carrier proteins are embedded in the inner membranes of mitochondria, where they transport solutes across the membrane. They belong to the SLC25 (solute carrier family 25) group of proteins [4]. Several members of the SLC25 group have been reported to play roles in GSIS (glucose-stimulated insulin secretion) in pancreatic $\beta$-cells. Overexpression or silencing of AGC1 (aspartate/glutamate carrier 1; SLC25A12 or Aralar1) has been reported to increase or reduce GSIS in INS-1E cells respectively [5,6]. Overexpression of UCP2 (uncoupling protein 2; SLC25A8) by adenovirus vector is known to inhibit GSIS from rat islets [7], whereas GSIS from islets of UCP2-deficient mice is enhanced compared with that from control islets [8]. In addition, down-regulation of OGC (2-oxoglutarate carrier; SLC25A11), CIC (citrate/isocitrate carrier; SLC25A1) and GC1 (glutamate carrier 1; SLC25A22) by siRNA (small interfering RNA) suppress GSIS [9–11].

The mitochondrial phosphate carrier PiC (SLC25A3) is a member of the SLC25 family and transports $P_i$ from the cytosol into the mitochondrial matrix. The *PiC* gene has 9 exons; the 3rd and the 4th exons are called exon 3A and exon 3B respectively. These two exons are alternatively spliced and two isoforms of PiC, PiC-A and PiC-B, are generated [12]. They differ considerably in their kinetic parameters as previously shown in a study using a reconstitution system [13]. The $K_m$ of PiC-A for $P_i$ on the external membrane surface is 3-fold that of PiC-B (PiC-A: ~2.2 mM; PiC-B: ~0.78 mM). The $K_m$ on the internal surface is much higher (PiC-A: ~9.7 mM; PiC-B: ~6.3 mM) than $K_m$ on the external membrane surface. The maximum transport rate of PiC-A is approximately a third that of PiC-B. These isoforms also differ in their tissue distribution. PiC-A is expressed in skeletal muscle and cardiac muscle, whereas PiC-B is expressed ubiquitously [13,14]. A case study of patients with PiC-A deficiency who suffered from lactic acidosis, heart failure and muscle weakness and died within the first year of life, demonstrates the critical significance of this carrier [15].

Since intramitochondrial $P_i$ is an essential substrate for mitochondrial ATP production by complex V (ATP synthase) and affects activity of the respiratory chain [16], the supply of $P_i$ from

Abbreviations used: AAC, ATP/ADP carrier; DAPP, diadenosine pentaphosphate; DIC, dicarboxylate carrier; FCCP, carbonyl cyanide *p*-trifluoromethoxyphenylhydrazone; GSIS, glucose-stimulated insulin secretion; KRBH, Krebs-Ringer bicarbonate Hepes buffer; RT, reverse transcription; siRNA, small interfering RNA; SLC25, solute carrier family 25; TMPD, *N*,*N*,*N*′,*N*′-tetramethyl-*p*-phenylenediamine.

[1] To whom correspondence should be addressed (email fujimoto@metab.kuhp.kyoto-u.ac.jp).

cytosol to mitochondrial matrix via PiC may be a rate-limiting step for ATP production. However, precise detection of PiC and its significance in metabolism–secretion coupling in pancreatic $\beta$-cells has not been reported previously. In the present study, the role of PiC in metabolism–secretion coupling in pancreatic $\beta$-cells is evaluated using INS-1 cells manipulated to reduce PiC expression.

## EXPERIMENTAL

### Materials

ATP, ADP, poly-L-ornithine, DAPP (diadenosine pentaphosphate), Safranin O, FCCP (carbonyl cyanide *p*-trifluoromethoxyphenylhydrazone), ATP sulfurylase and $Na_2MoO_4$ were purchased from Sigma. Hepes, KCl, EGTA, sodium pyruvate, $MgSO_4$, $NaH_2PO_4$, $CaCl_2$, glucose, NaCl, $NaHCO_3$, $HClO_4$, $Na_2CO_3$, pyruvate kinase, BSA, KOH, potassium gluconate and $KH_2PO_4$ were purchased from Nacalai. 2-mercaptoethanol, penicillin, streptomycin and mouse monoclonal antibodies to the subunits of the mitochondrial respiratory chain complexes were purchased from Invitrogen. Luciferin-luciferase was purchased from Promega.

### Cell culture

INS-1 (rat insulinoma) cells were cultured in RPMI 1640 medium containing 11.1 mM glucose (Invitrogen) supplemented with 10 % heat-inactivated fetal calf serum, 10 mM Hepes, 2 mM L-glutamine, 1 mM sodium pyruvate, 50 $\mu$M 2-mercaptoethanol, 100 IU/ml penicillin and 100 $\mu$g/ml streptomycin at 37 °C in a humidified atmosphere (5 % $CO_2$ and 95 % air). COS-7 (African green monkey kidney) cells were cultured in Dulbeco's modified Eagle's medium supplemented with 10 % heat-inactivated fetal calf serum, 100 IU/ml penicillin and 100 $\mu$g/ml streptomycin at 37 °C in a humidified atmosphere (5 % $CO_2$ and 95 % air).

### siRNA transfection

Stealth™ siRNAs were synthesized by Invitrogen. The sequences of siRNAs specific for both rat PiC-A and PiC-B were: 5′-AAAUAUGCCCUUGUACUUCUGAGGG-3′ and 5′-CCCUCAGAAGUACAAGGGCAUAUUU-3′ designated as PiC siRNA1 and 5′-GAACACCUAUCUGUGGCGUACAUCA-3′ and 5′-UGAUGUACGCCACAGAUAGGUGUUC-3′ designated as PiC siRNA2. The sequences of control siRNAs were: 5′-ACCAACAACAGUUUGGGAAUAGGGA-3′ and 5′-UCCCUAUUCCCAAACUGUUGUUGGU-3′. Cultured INS-1 cells were trypsinized, suspended with RPMI 1640 medium without antibiotics, mixed with Opti-MEM (Invitrogen) containing siRNA and Lipofectamine™ 2000 (Invitrogen), plated on dishes or wells and then incubated at 37 °C in a $CO_2$ incubator. The final amounts of INS-1 cells, RPMI 1640, Opti-MEM, siRNA and Lipofectamine™ 2000 were $1\times10^6$ cells/ml, 75 % (v/v), 25 % (v/v), 80 nM and 0.3 % respectively. Medium was replaced with RPMI 1640 3–4 h after transfection. All experiments using siRNA-transfected INS-1 cells were performed 48 h after transfection unless otherwise noted.

### Isolation of total RNA and quantitative RT (reverse transcription)–PCR

Total RNA was isolated from cardiac muscle, brain, skeletal muscle, kidney, liver and lung of Wistar rats using TRIzol® (Invitrogen) and from islets of Wistar rats and INS-1 cells using RNeasy mini kit (Qiagen). Animals were maintained and used in accordance with the Guidelines for Animal Experiments of Kyoto University. Islets were isolated by collagenase digestion [17]. cDNA was prepared by reverse transcriptase (Superscript II; Invitrogen) with an oligo(dT) primer. The rat sequences of forward and reverse primers to detect PiC-A, PiC-B, total PiC (PiC-A plus PiC-B) and $\beta$-actin (as an inner control) are shown in Table 1. AmpliTaq Gold (Applied Biosystems) was used as a DNA polymerase for RT–PCR. SYBR Green PCR Master Mix (Applied Biosystems) was prepared for the quantitative RT–PCR run. The thermal cycling conditions were denaturation at 95 °C for 10 min followed by 40 cycles at 95 °C for 30s and 60 °C for 30s.

**Table 1 Primer sequences used in RT–PCR and quantitative RT–PCR**

| Name | Forward | Reverse |
|---|---|---|
| PiC-A | 5′-AGCTGGTGCACGATGTGTCG-3′ | 5′-TTCCTCCGAGTCCACAGAGG-3′ |
| PiC-B | 5′-AGCTGGTGCACGATGTGTCG-3′ | 5′-CCACCAAAGCCACACAGTGC-3′ |
| Total PiC (PiC-A+PiC-B) | 5′-AGAGCAGCTGGTTGTGACAT-3′ | 5′-ACACCTCTAAAGCCAAGCCT-3′ |
| $\beta$-actin | 5′-CAATGAGCGGTTCCGATGCC-3′ | 5′-AATGCCTGGGTACATGGTGG-3′ |

### Plasmid construction and transfection

The cDNA fragment of rat PiC-B was obtained from rat islets by RT–PCR and cloned into the pHMCA5 vector. pHMCA5-PiC-B was transfected into COS-7 and INS-1 cells using FuGENE™ 6 transfection reagent (Roche) and Lipofectamine™ 2000 respectively.

### Immunoblot analysis

Rabbit antibody against the rat PiC peptide PPEM-PESLKKKLGLTE corresponding to C-terminal residues was originally raised. For immunoblotting, cells were washed with PBS containing protease inhibitor (Complete; Roche), suspended in 1 ml of PBS containing protease inhibitor and homogenized. Protein (50 $\mu$g per sample) was separated on a 15 % polyacrylamide gel and transferred to a nitrocellulose membrane. After blocking with TBS (Tris-buffered saline; 10 mM Tris/HCl and 100 mM NaCl, pH 7.5) containing 0.1 % Tween 20 and 5 % skimmed milk (blocking buffer) at room temperature (25 °C) for 2 h, blotted membranes were incubated overnight at 4 °C with anti-PiC antibody at 1:500 dilution, anti-DIC (dicarboxylate carrier) antibody (Novus Biologicals) at 1:100 dilution, mouse monoclonal anti-complex I (39 kDa subunit) antibody, anti-complex III (core II) antibody, anti-complex IV (subunit I) antibody or anti-complex V (subunit $\alpha$) of mitochondrial respiratory chain antibody at 1:1000 dilution in blocking buffer, and subsequently with anti-rabbit (for PiC and DIC) or anti-mouse (for respiratory chain proteins) IgG horseradish peroxidase-conjugated secondary antibody (GE Healthcare) diluted 1:5000 at room temperature for 2 h prior to detection using ECL (GE Healthcare). In the same membrane, the process was repeated for $\beta$-actin at 1:1000 dilution of the antibody. Band intensities were quantified with Multi Gauge software (Fujifilm).

### Insulin secretion

For insulin secretion assays, INS-1 cells cultured on 24-well plates coated with 0.001 % poly-L-ornithine were washed with KRBH (Krebs-Ringer bicarbonate Hepes buffer) composed of

140 mM NaCl, 3.6 mM KCl, 0.5 mM $MgSO_4$, 0.5 mM $NaH_2PO_4$, 1.5 mM $CaCl_2$, 2 mM $NaHCO_3$, 0.1 % BSA and 10 mM Hepes (pH 7.4) with 2 mM glucose, preincubated at 37 °C for 30 min in KRBH with 2 mM glucose, and then incubated at 37 °C for 30 min in KRBH with 2 mM glucose, 10 mM glucose or 2 mM glucose plus 30 mM KCl. Insulin concentrations were determined by RIA using rat insulin as a standard as previously described [17].

### Adenine nucleotides

ATP and ADP contents were determined as previously described [18,19] with some modifications. Briefly, INS-1 cells were cultured, washed and preincubated as described above and incubated with KRBH with 2 mM glucose, 10 mM glucose or 2 mM glucose plus 30 mM KCl at 37 °C for 30 min. Incubation was stopped by the addition of $HClO_4$. The contents of wells were sonicated [three pulses of 3 s duration using a Handy Sonic UR-20P instrument (TOMY SEIKO) on ice] and transferred into glass tubes. The tubes were then centrifuged, and a fraction of the supernatant was neutralized with Hepes and $Na_2CO_3$. The ATP concentration was measured by luciferin-luciferase assay. After ATP in the neutralized extract was irreversibly converted to AMP with ATP sulfurylase in the presence of $Na_2MoO_4$, ADP in the reactant was converted to ATP with pyruvate kinase and was determined by luciferin-luciferase assay as the difference between the measurements with and without pyruvate kinase.

### Intracellular calcium concentration ($[Ca^{2+}]_i$) and mitochondrial membrane potential ($\Delta\psi_m$) in living cells

INS-1 cells were seeded on to glass coverslips coated with 0.001 % poly-L-ornithine and cultured 48 h before measurements were made. For measurements of $[Ca^{2+}]_i$, cultured INS-1 cells were loaded with 5 $\mu$M Fura-PE3/AM (Calbiochem) at 37 °C for 90 min, placed in a heat-controlled chamber on the stage of an inverted microscope kept at 36 ± 1 °C, superfused with KRBH containing 2 mM glucose, and subsequently exposed to the buffer containing 10 mM glucose or 30 mM KCl. The cells were excited successively at 340 and 380 nm, and the fluorescence emitted at 510 nm was captured by CCD camera (Micro Max 5 MHz System, Roper Industries, Trenton, NJ). The images were analysed with the Meta Fluor image analyzing system (Universal Imaging). The 340 nm (F340) and 380 nm (F380) fluorescence signals were detected every 15 s, and ratios (F340/F380) were calculated. For $\Delta\psi_m$ measurements, the same protocol as above was used except that cultured cells were loaded with 10 $\mu$g/ml rhodamine 123 (Invitrogen) at 37 °C for 30 min and fluorescence excited at 490 nm and emitted at 530 nm every 20 s was monitored.

### ATP production and $\Delta\psi_m$ in mitochondrial fraction

Measurement of ATP production from the mitochondrial fraction was performed as previously described [18] with minor modifications. Firstly, INS-1 cells were homogenized in solution A consisting of 50 mM Hepes, 100 mM KCl, 1.8 mM ATP, 1 mM EGTA, 2 mM $MgCl_2$ and 0.5 mg/ml BSA (electrophoretically homogeneous) with the pH adjusted to 7.00 at 37 °C with KOH. After precipitation of cell debris and nuclei by 800 *g* centrifugation for 3 min, the supernatant was centrifuged more rapidly (10000 *g* for 3 min) to obtain a pellet containing the mitochondrial fraction. The precipitation, diluted by 200 $\mu$l of solution A, was centrifuged again and rinsed three times in solution B, consisting of 20 mM Hepes, 1 mM EGTA, 12 mM NaCl, 0.3 mM $MgCl_2$, 130 mM potassium gluconate and 0.5 mg/ml BSA (electrophoretically homogeneous) with the pH adjusted to 7.10 with KOH. The mitochondrial fraction in 500 $\mu$l of solution B was kept on ice until use. To measure ATP production by oxidative phosphorylation, the reaction was started by adding mitochondrial suspension to prewarmed solution B (37 °C) containing mitochondrial substrates with or without respiratory chain inhibitors, 50 $\mu$M ADP, 1 $\mu$M DAPP and various levels of $P_i$. DAPP, a specific inhibitor of adenylate kinase, was used to measure ATP production by oxidative phosphorylation exclusively. After the reaction was stopped, the ATP concentration in the solutions was measured by adding luciferin-luciferase solution with a bioluminometer. ATP production was corrected by mitochondrial protein content. Measurement of $\Delta\psi_m$ was performed as previously described [20] with some modifications. Fluorescence was successively monitored using a spectrofluorophotometer (RF 5000; Shimadzu) with an excitation wavelength of 495 nm and emission at 586 nm, and with stirring solution B supplemented with 3 mM $KH_2PO_4$, 50 $\mu$M ADP and 2.5 $\mu$M Safranin O applied in a glass cuvette at 37 °C. Mitochondria, succinate and FCCP were added to the solution in this order and final concentrations were 50 $\mu$g/ml, 1 mM and 200 nM respectively.

### Statistical analysis

The data are expressed as means ± S.E.M. Statistical significance was calculated by unpaired Student's *t* test. $P < 0.05$ was considered significant.

## RESULTS

### Expression of PiC mRNA in pancreatic $\beta$-cells

Tissue distribution of PiC was evaluated by RT–PCR (Figure 1A). PiC-B was expressed ubiquitously whereas PiC-A was expressed clearly in cardiac muscle and skeletal muscle as previously reported [13,14] and obscurely in rat islets and INS-1 cells. These results indicate that PiC-B was dominantly expressed in pancreatic $\beta$-cells.

### Evaluation of anti-PiC antibody

The cell lysates of COS-7 cells transfected with pHMCA5-PiC or pHMCA5-null, INS-1 cells transfected with pHMCA5-null, intact INS-1 cells and rat islets were electrophoresed and immunoblotted using the anti-PiC antibody. As shown in Figure 1(B), the band at ~30 kDa, which was not detected in COS-7 cells transfected with pHMCA5-null, was detected in COS-7 cells transfected with pHMCA5-PiC, INS-1 cells transfected with pHMCA5-null, intact INS-1 cells and rat islets. This observation is consistent with a previous report that rat PiC was detected at ~30 kDa by an antibody originally raised using the C-terminal amino acids as the antigen peptide [21].

### Silencing effects of PiC siRNAs on INS-1 cells

Quantitative RT–PCR assays using primers for total PiC (PiC-A plus PiC-B, Table 1) and immunoblotting using anti-PiC antibody revealed ~70 % reduction of PiC mRNA expression and ~40 % reduction of the protein expression in INS-1 cells 48 h after both PiC siRNA1 and 2 transfection respectively (Figures 1C and 1D). Time-dependent reduction of PiC protein expression (~25 %, ~40 % and ~50 % reduction at 24 h, 48 h and 72 h after siRNA1 and 2 transfection) implies long half-life of PiC, which causes low efficacy of suppression (Figure 1D). Transfection of control siRNA did not affect the expression of PiC in INS-1 cells at both mRNA and protein levels. Protein expressions of DIC,

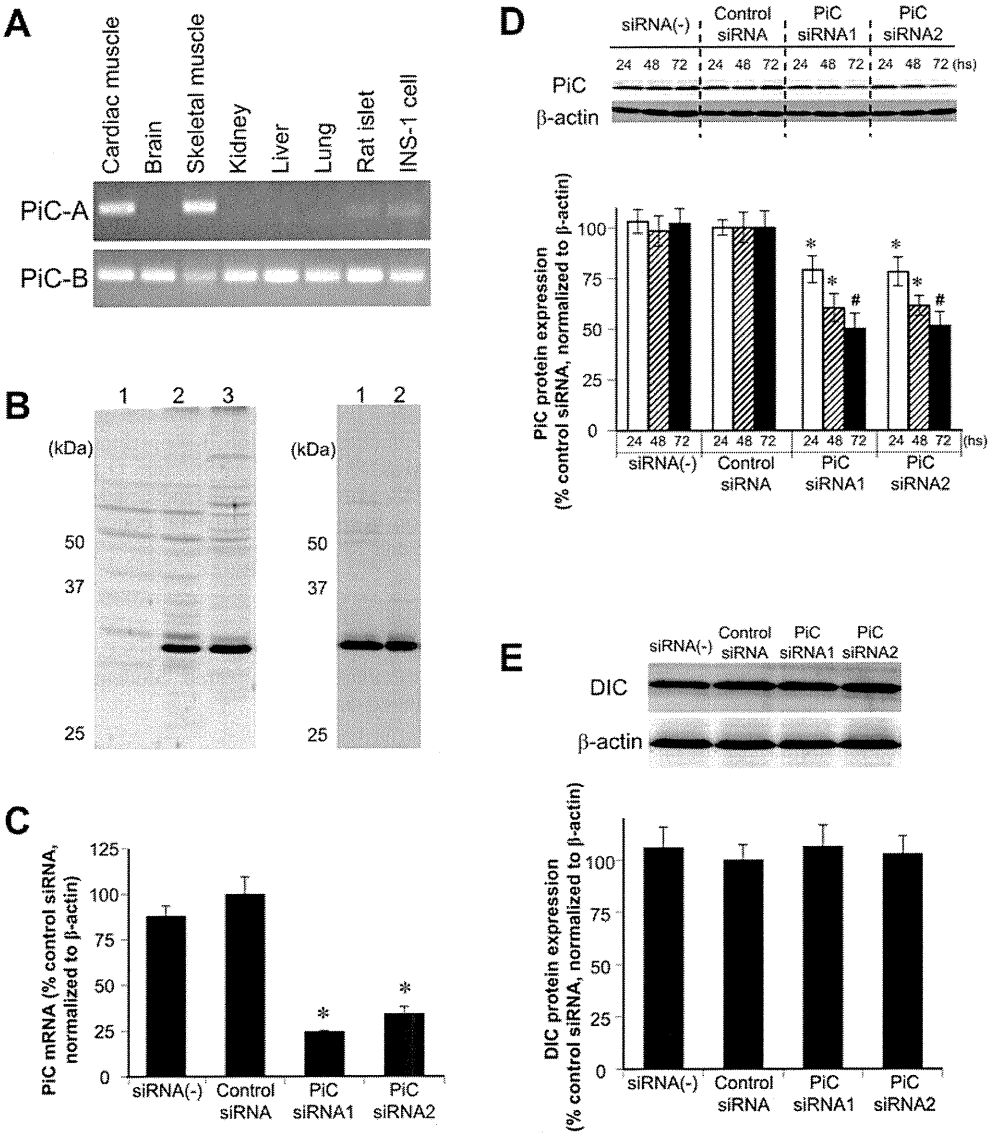


**Figure 1 Detection of rat PiC and silencing effects of PiC siRNAs on INS-1 cells**

(**A**) RT–PCR detection of PiC mRNA expression in various rat tissues and INS-1 cells. PiC mRNA expressions in cardiac muscle, brain, skeletal muscle, kidney, liver, lung and islets of Wistar rat and INS-1 cells were evaluated with RT–PCR using primers of specific sequences for PiC-A and PiC-B. Product sizes are 141 bp for PiC-A and 136 bp for PiC-B. (**B**) Evaluation of anti-PiC antibody by immunoblot analysis. Left panel: whole cell lysates from COS-7 cells transfected with pHMCA5-null (lane 1), COS-7 cells transfected with pHMCA5-PiC (lane 2) and INS-1 cells transfected with pHMCA5-null (lane 3) were electrophoresed and immunoblotted with anti-PiC antibody. Right panel: whole cell lysates from INS-1 cells (lane 1) and rat islets (lane 2) were electrophoresed and immunoblotted with anti-PiC antibody. Molecular mass in kDa is given on the left-hand side of each panel. (**C**) Effects of transfection of PiC siRNAs on the expression of PiC mRNA was evaluated with quantitative RT–PCR using a pair of primers recognizing both PiC-A and PiC-B (total PiC). Data were normalized using $\beta$-actin mRNA. $n = 3$ in each group. $^*P < 0.01$ compared with control siRNA. (**D**) Immunoblot analysis of PiC expression revealed that PiC siRNAs reduced PiC expression in INS-1 cells. Time (h) after siRNA transfection is indicated. Data were normalized by the expression of $\beta$-actin. $n = 4$ in each bar. $^*P < 0.05$ and $\#P < 0.01$ compared with control siRNA. (**E**) Effects of PiC silencing on expression of DIC. Whole INS-1 cell lysate was electrophoresed and immunoblotted using antibodies against DIC. Quantification data were obtained from four independent experiments and normalized with $\beta$-actin levels.

another $P_i$ carrier, were not affected by siRNA1 and 2 transfection (Figure 1E).

### Effects of PiC down-regulation on glucose- and depolarization-stimulated insulin secretion

Down-regulation of PiC decreased GSIS (10 mM glucose) in INS-1 cells, as shown in Figure 2. A reduction in GSIS of 61 % by PiC siRNA1 and 47 % by PiC siRNA2 was observed. $K^+$ (30 mM)-stimulated insulin secretion was also reduced: the reduction was 27 % by PiC siRNA1 and 23 % by PiC siRNA2, which were milder than those of GSIS (Figure 2). Insulin secretion in the basal glucose state (2 mM) was not affected by PiC siRNA1, but was slightly increased by PiC siRNA2. Transfection of control siRNA did not affect GSIS in INS-1 cells.

### Effects of PiC down-regulation on adenine nucleotides

Down-regulation of PiC increased ADP and decreased the ATP:ADP ratio, whereas it did not significantly affect ATP in

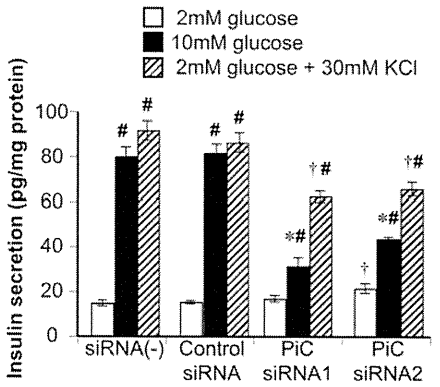


**Figure 2 Effects of PiC down-regulation on glucose- or KCl-stimulated insulin secretion**

INS-1 cells were incubated for 30 min with 2 mM glucose, 10 mM glucose or 2 mM glucose and 30 mM $K^+$, and insulin secretion was measured. Data were obtained from six independent experiments normalized by protein concentration. Error bars are means ± S.E.M. *$P < 0.01$ and †$P < 0.05$ compared with control siRNA at the corresponding condition. #$P < 0.01$ compared with corresponding 2 mM glucose.

the presence of 10 mM glucose in INS-1 cells (Table 2A). ATP, ADP and the ATP:ADP ratio at 2 mM glucose was not altered by silencing PiC (Tables 2A and 2B). Depolarization evoked by 30 mM $K^+$ in the presence of 2 mM glucose decreased the ATP:ADP ratio in both control and PiC down-regulated cells, whereas suppression of the ATP:ADP ratio was lower in PiC down-regulated cells compared with control cells (Table 2B).

### Effects of PiC down-regulation on $[Ca^{2+}]_i$ and $\Delta\psi_m$ in living cells

Fluorescence signals of Fura-PE3 revealed that elevation of $[Ca^{2+}]_i$ in response to a stimulating level of 10 mM glucose was decreased and delayed by PiC down-regulation compared with that in control (Figure 3A). Average values calculated using the data from Figure 3(A) also indicate that PiC siRNA reduced the mean $[Ca^{2+}]_i$ at 10 mM glucose (PiC siRNA1, $0.864 \pm 0.004$ compared with control siRNA, $0.896 \pm 0.003$; $P < 0.01$) whereas there was no significant change at basal (2 mM) glucose (PiC siRNA1, $0.846 \pm 0.004$; control siRNA, $0.857 \pm 0.003$), as shown in Figure 3(B). Elevation of $[Ca^{2+}]_i$ in response to 30 mM $K^+$ was slightly decreased by PiC siRNA1 (average value of Fura-PE3 fluorescence ratio was $0.968 \pm 0.005$, compared with a control siRNA ratio of $0.991 \pm 0.005$, $P < 0.01$) without affecting basal value (control siRNA, $0.857 \pm 0.006$; siRNA1, $0.854 \pm 0.004$) as shown in Figures 3(C) and 3(D). Fluorescence measurement using rhodamine 123 demonstrated that the mitochondrial membrane in INS-1 cells was hyperpolarized by raising glucose from 2 to 10 mM and prominently depolarized by FCCP, and that PiC down-regulation did not affect glucose-induced hyperpolarization and total depolarization after FCCP exposure of $\Delta\psi_m$ throughout the measurement (Figure 3E).

### Effects of PiC down-regulation on ATP production and $\Delta\psi_m$ in mitochondrial fraction

ATP production by mitochondria from INS-1 cells transfected with control or PiC siRNAs in the presence of 1 mM succinate and various concentrations of $P_i$ ($[P_i]$) is shown in Figure 4(A). PiC down-regulation decreased mitochondrial ATP production by 50–60 % at $[P_i]$ ranging from 0.001 to 10 mM. ATP production in all groups reached maximum rates above ~3 mM of $[P_i]$, which indicates that the PiC amount regulates the maximal rate of mitochondrial ATP production. On the other hand, $K_m$ values of $[P_i]$ for ATP production were similar (~0.05 mM). Mitochondrial ATP production in the presence of various mitochondrial substrates and inhibitors of the respiratory chain is shown in Table 3. ATP production in the presence of succinate was completely inhibited by antimycin A, a complex III inhibitor, in both control and PiC down-regulated INS-1 cells. PiC siRNAs decreased ATP production in the presence of pyruvate and malate by 42–58 %, succinate plus rotenone by 46–62 % and TMPD (*N*,*N*,*N*′,*N*′-tetramethyl-*p*-phenylenediamine) plus ascorbate by 61–62 %, showing that ATP production by electrons rendered at complex I, complex II and complex IV is suppressed to a similar degree. In spite of significant down-regulation of ATP production, PiC down-regulation did not affect $\Delta\psi_m$ of isolated mitochondria measured with Safranin O in the presence of succinate (Figure 4B).

### Effects of PiC down-regulation on expression of mitochondrial respiratory chain proteins

Immunoblotting using lysates of whole INS-1 cells revealed that transfection of PiC siRNAs did not change the expression of complex I, III, IV or V of mitochondrial respiratory chain proteins (Figure 5).

## DISCUSSION

In the present study, the mitochondrial phosphate carrier (PiC) was revealed to play an important role in metabolism–secretion coupling of pancreatic β-cells by using INS-1 cells and PiC siRNA. PiC down-regulation brings about reduction in mitochondrial ATP production by mitochondrial fuels, resulting in reduced glucose-induced $[Ca^{2+}]_i$ elevation and impaired GSIS.

In pancreatic β-cells, ATP increase is slight and ADP decrease is prominent via an increase in glucose levels beyond the triggering level of insulin secretion. In addition, the ATP/ADP ratio is well-correlated with GSIS rather than the absolute value of ATP [22,23]. PiC down-regulation decreased the ATP/ADP ratio in the presence of high glucose, which causes insufficient closure of $K_{ATP}$ channels, a decrease in $[Ca^{2+}]_i$ elevation by glucose (Figures 3A and 3B), and suppression of GSIS (Figure 2).

Insulin secretion at 10 mM glucose was similar to that at 30 mM $K^+$ and 2 mM glucose in the control samples. In contrast, in PiC down-regulated INS-1 cells, GSIS is lower than depolarization-induced insulin secretion, which suggests specific effects of PiC on metabolism–secretion coupling (Figure 2). However, ~25 % suppression of depolarization-induced insulin secretion, which is modest compared with GSIS, was observed in PiC down-regulated INS-1 cells. Measurements revealed that $[Ca^{2+}]_i$ in the presence of 2 mM glucose and 30 mM $K^+$ was reduced by PiC down-regulation (Figures 3C and 3D), which plays a role in reduced depolarization-induced insulin secretion by PiC down-regulation. Depolarization reduced the ATP/ADP ratio in the presence of a basal level of glucose in control samples, which accords with a previous study where an increase in $[Ca^{2+}]_i$ causes a larger consumption than production of ATP [24] (Table 2B). The ATP/ADP ratio was also reduced by depolarization at 2 mM glucose in PiC down-regulated INS-1 cells, although the suppression was lower than that in control samples, which may reflect a smaller elevation of $[Ca^{2+}]_i$ than in the control. In addition, in contrast with a significant suppression of the ATP/ADP ratio at high glucose concentrations by PiC down-regulation, in the presence of a basal

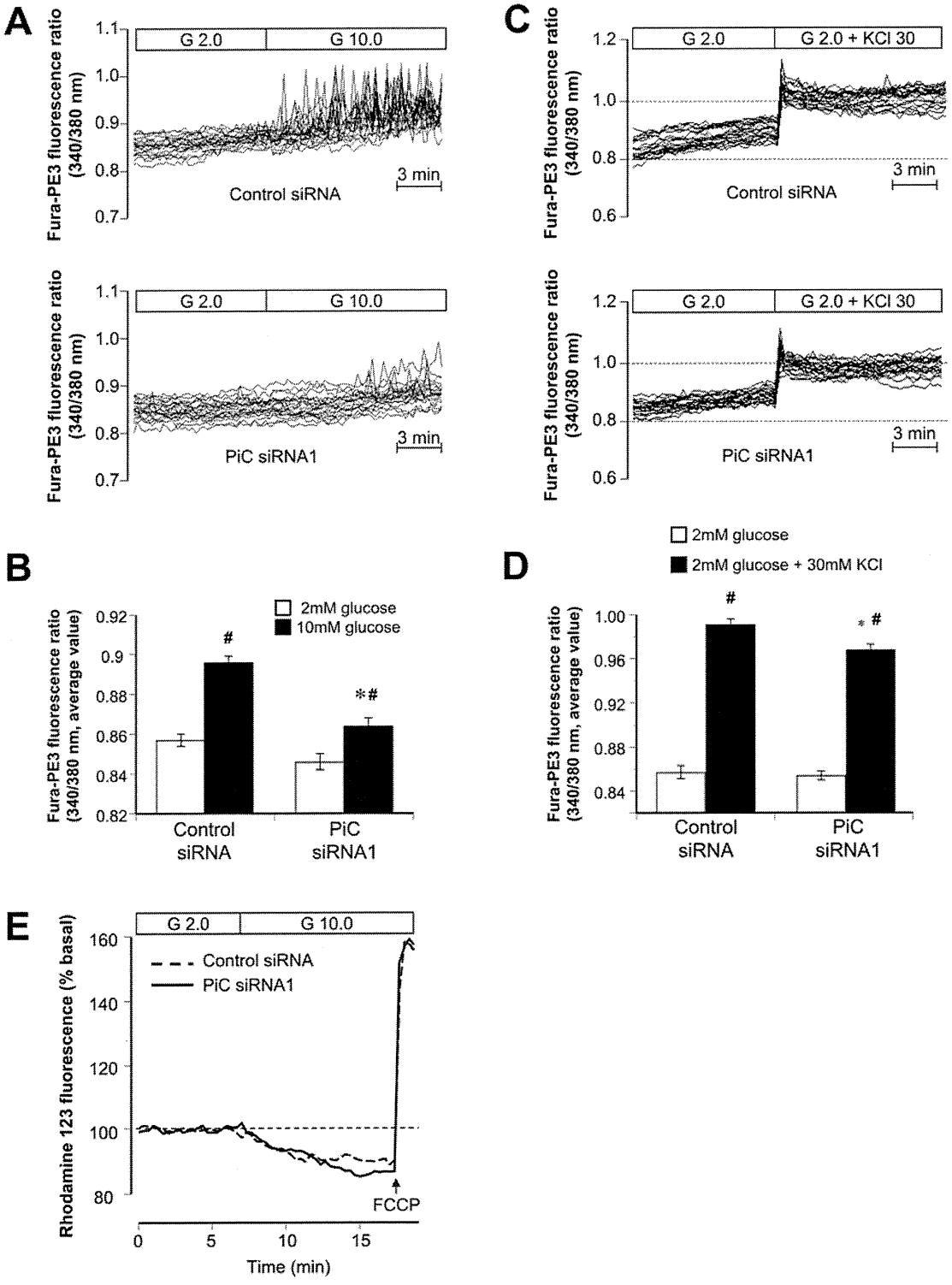


**Figure 3 Effects of PiC down-regulation on $[Ca^{2+}]_i$ and $\Delta\psi_m$ in living cells**

(**A**) $[Ca^{2+}]_i$ elevation and oscillation induced by raising glucose (G) from 2 to 10 mM were monitored in INS-1 cells transfected with PiC siRNA. Traces of Fura-PE3 fluorescence ratio (340/380 nm) were obtained from 20 cells of each group. (**B**) Average values calculated from the data from (**A**). $*P < 0.01$ compared with control siRNA at 10 mM glucose. $\#P < 0.01$ compared with corresponding 2 mM glucose. (**C**) $[Ca^{2+}]_i$ elevation induced by 30 mM KCl was monitored in INS-1 cells transfected with PiC siRNA. Traces of Fura-PE3 fluorescence ratio (340/380 nm) were obtained from 20 cells of each group. (**D**) Average values calculated from the data from (**C**). $*P < 0.05$ compared with control siRNA at 30 mM KCl. $\#P < 0.01$ compared with corresponding 2 mM glucose. (**E**) $\Delta\psi_m$ monitored by rhodamine 123 fluorescence in INS-1 cells. Data were corrected with the average values of fluorescence under basal glucose (2 mM) conditions. $n = 10$. Error bars are means±S.E.M.

**Table 2 Effects of PiC down-regulation on adenine nucleotides**

(A)

| | Control siRNA | | PiC siRNA1 | | PiC siRNA2 | |
|---|---|---|---|---|---|---|
| Glucose (mM) | 2 | 10 | 2 | 10 | 2 | 10 |
| ATP (nmol/mg protein) | 65.2 ± 3.8 | 77.4 ± 3.8* | 64.4 ± 1.0 | 71.8 ± 3.3* | 66.2 ± 1.7 | 80.0 ± 5.5* |
| ADP (nmol/mg protein) | 10.2 ± 0.6 | 3.9 ± 0.4† | 10.6 ± 0.6 | 6.4 ± 0.9*‡ | 9.7 ± 0.6 | 6.1 ± 1.2*‡ |
| ATP/ADP | 6.5 ± 0.6 | 20.5 ± 2.0† | 6.1 ± 0.4 | 12.0 ± 1.7*‡ | 6.9 ± 0.5 | 13.9 ± 1.4*‡ |

(B)

| | Control siRNA | | | PiC siRNA1 | |
|---|---|---|---|---|---|
| Glucose (mM) | 2 | 2 | 2 | 2 | 2 |
| $K^+$ (mM) | 3.6 | 30 | 3.6 | 3.6 | 30 |
| Antimycin A ($\mu$M) | 0 | 0 | 1 | 0 | 0 |
| ATP (nmol/mg protein) | 65.5 ± 3.4 | 48.6 ± 1.9* | 2.5 ± 0.1† | 64.4 ± 4.7 | 61.2 ± 1.8‡ |
| ADP (nmol/mg protein) | 10.1 ± 0.1 | 11.2 ± 0.2* | 10.5 ± 0.1* | 9.9 ± 0.2 | 10.5 ± 0.3*‡ |
| ATP/ADP | 6.5 ± 0.3 | 4.4 ± 0.2† | 0.2 ± 0.0† | 6.5 ± 0.5 | 5.8 ± 0.2*§ |

*$P < 0.05$ and †$P < 0.01$ compared with basal condition (2 mM glucose). ‡$P < 0.05$ and §$P < 0.01$ compared with control siRNA. Data were obtained from four independent experiments.

**Table 3 Silencing effects of PiC siRNAs on ATP production from mitochondrial fraction of INS-1 cells**

| | Mitochondrial ATP production ($\mu$mol/10 min per mg of protein) | | |
|---|---|---|---|
| Experimental conditions | Control siRNA | PiC siRNA1 | PiC siRNA2 |
| 1 mM succinate | 1.28 ± 0.02 | 0.61 ± 0.02* | 0.46 ± 0.01* |
| 1 mM succinate + 1 $\mu$M rotenone | 1.03 ± 0.09 | 0.56 ± 0.03* | 0.39 ± 0.01* |
| 1 mM succinate + 1 $\mu$M antimycin A | 0.03 ± 0.01 | 0.00 ± 0.01 | 0.00 ± 0.01 |
| 1 mM pyruvate + 1 mM malate | 0.41 ± 0.03 | 0.24 ± 0.01* | 0.17 ± 0.00* |
| 0.5 mM TMPD + 2 mM ascorbate | 3.43 ± 0.09 | 1.33 ± 0.03* | 1.27 ± 0.01* |

*$P < 0.01$ compared with control siRNA. Data were obtained from three independent experiments.

level of glucose, PiC down-regulation did not affect the ATP/ADP ratio in INS-1 cells. An incomplete compensatory effect derived from PiC down-regulation, which is valid in a basal supply of substrate to mitochondria but deteriorates in an accelerated supply at high glucose, might save ATP consumption and maintain the basal ratio of ATP/ADP.

PiC, which is required for mitochondrial ATP production, has two isoforms. PiC-A is expressed in skeletal and cardiac muscle whereas PiC-B is expressed ubiquitously. AAC (ATP/ADP carrier), which is also required for mitochondrial ATP production, has isoforms including AAC1 (SLC25A4), AAC2 (SLC25A5) and AAC3 (SLC25A6). Interestingly, these isoforms, except AAC2, expression of which is absent or scarce in most tissues, distribute similarly to the PiC isoforms: AAC1 is expressed in skeletal and cardiac muscle, and AAC3 is expressed ubiquitously. These distributions imply that ubiquitously-expressed PiC-B and AAC3 may meet stable energy requirement, and PiC-A and AAC1, which are expressed exclusively in muscle, meet higher and prompt energy demands for muscle contraction. In the present study, we demonstrate that PiC-B is the dominant isoform of PiC whereas PiC-A is scarcely expressed in INS-1 cells and rat islets (Figure 1A), which may reflect less prompt energy demand in $\beta$-cells compared with that in muscles.

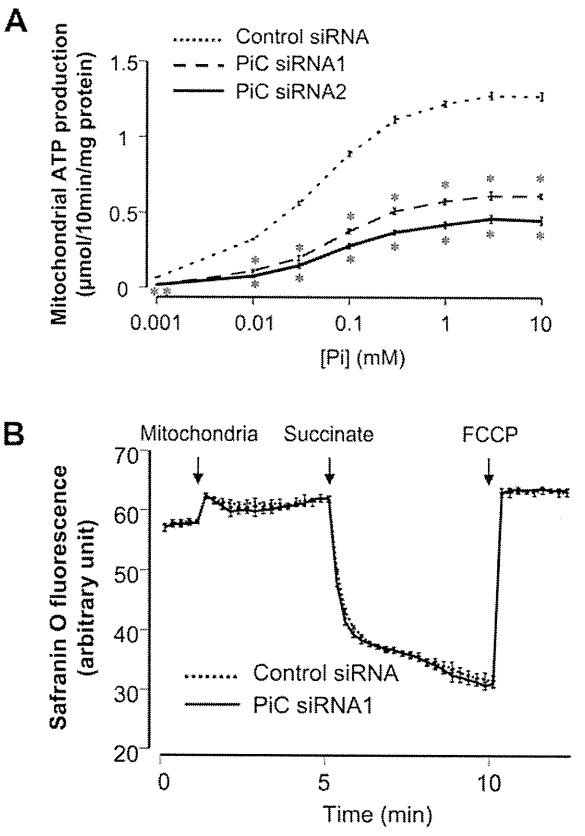


**Figure 4 Effects of PiC down-regulation on ATP production and $\Delta\psi_m$ in mitochondrial fraction isolated from INS-1 cells**

(**A**) Effects of PiC down-regulation on mitochondrial ATP production at various phosphate concentrations. ATP production was evaluated in mitochondria isolated from INS-1 cells in the presence of 50 $\mu$M ADP, 1 $\mu$M DAPP and 1 mM succinate with various concentrations of $P_i$ indicated in the Figure. $n = 3$ in each plot. *$P < 0.01$ compared with control siRNA. (**B**) $\Delta\psi_m$ monitored by Safranin O fluorescence. Mitochondria (50 $\mu$g/ml), succinate (1 mM) and FCCP (200 nM) were added to the solution containing Safranin O at the points indicated with arrows. $n = 4$ in each group.

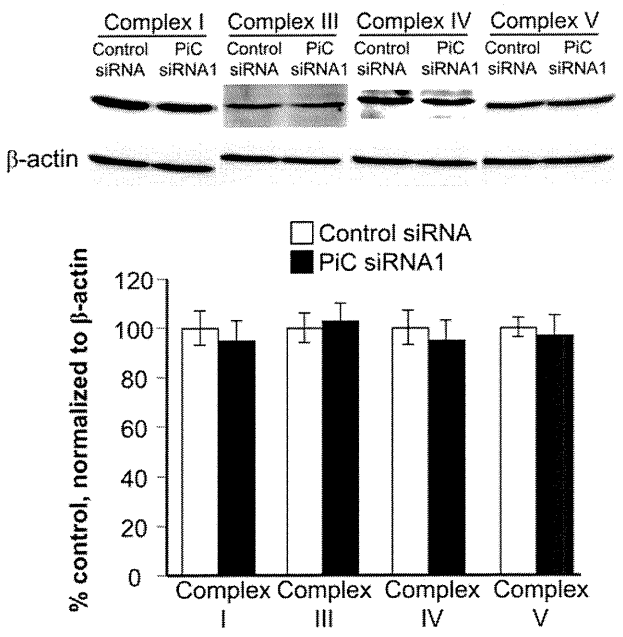


**Figure 5 Effects of PiC silencing on expression of mitochondrial respiratory chain proteins**

Lysates of whole INS-1 cells were electrophoresed and immunoblotted using antibodies against complex I, III, IV and V. Quantification data were obtained from four independent experiments and normalized with $\beta$-actin levels. Error bars are means±S.E.M.

Mitochondrial ATP is produced by complex V (ATP synthase), which is driven by protonmotive force generated by proton extrusion during transport of high-energy electrons in the respiratory chain. In the present study, mitochondrial ATP production in the presence of mitochondrial fuel increased according to the raised extramitochondrial phosphate concentration ($[P_i]_e$), and reached maximum rate above ~3 mM of $[P_i]_e$, which was decreased by 50–60 % without affecting the $K_m$ value of $[P_i]_e$ for ATP production by ~40 % reduction in PiC protein. The physiological intracellular $[P_i]$ in heart determined by methods including $^{31}P$ NMR is ~1 mM at rest and increases to ~10 mM depending on the metabolic state [25–27]. Levels of $P_i$ in islets are ~20 mmol/kg of dry weight tissue [28], which corresponds to ~10 mM by conversion [29]. Taken together, the rate of mitochondrial ATP production might be barely affected by a physiological change of $[P_i]_e$ but be evidently affected by alteration of the amount of PiC protein. In addition, reduction in ATP production by down-regulation of PiC also suggests that compensatory supply of $P_i$ to mitochondria by other mitochondrial phosphate carriers including DIC (SLC25A10) [30,31] does not occur, which is supported by no apparent effect of PiC down-regulation on DIC expression (Figure 1E). These results accord with the first description that PiC dysfunction impairs the synthesis of ATP [15].

Intramitochondrial $P_i$ is thought to affect oxidative phosphorylation at multiple sites [16]. To find specific defective sites in the respiratory chain in PiC down-regulated INS-1 cells, mitochondrial ATP production was examined in the presence of various substrates and inhibitors. Pyruvate and malate, which are metabolized in mitochondria to generate NADH, render electrons at complex I. In the presence of rotenone, a complex I inhibitor, succinate renders electrons directly to complex II via $FADH_2$. TMPD is an artificial electron donor that can transfer electrons to cytochrome *c*. TMPD reduced by ascorbate renders electrons to cytochrome *c*, which transfers electrons to complex IV. Reduction of ATP production by down-regulation of PiC in the presence of pyruvate plus malate, succinate plus rotenone and TMPD plus ascorbate were all suppressed similarly by 50–60 % (Table 3). These results indicate that reduction in ATP production by down-regulation of PiC may well be derived from a defective site downstream of complex IV and that a defective site upstream of complex IV, if present, does not play a prominent role. Moreover, immunoblotting revealed that expressions of respiratory chain proteins including complex I, III, IV and V were not affected by PiC silencing. Considered together, silencing of PiC seems to suppress mitochondrial ATP production not by affecting mitochondrial biogenesis, but by restricting $P_i$ supply to complex V.

Inhibition of complex V by oligomycin reduces ATP production with hyperpolarization of $\Delta\psi_m$ [32,33], which may be derived from the fact that complex V is a protonophore and its inhibition affects electrogenic $H^+$ influx to mitochondria specifically and directly affects $\Delta\psi_m$. In contrast, PiC is electroneutral due to symport of $H^+$ and negatively charged $P_i$ or antiport of $OH^-$ and negatively charged $P_i$ and does not directly affect $\Delta\psi_m$. ATP generation in complex V is driven by protonmotive force ($\Delta p$), which has two components: electrical membrane potential ($\Delta\psi_m$) and the difference between the cytosolic and matrix pH ($\Delta pH$) [34,35]. $P_i$ plays regulatory roles in oxidative phosphorylation by affecting $\Delta p$. An increase in $[P_i]_e$ reduces $\Delta pH$ [34,36–38] due to an increase in co-transport of $P_i$ and protons from cytosol into mitochondrial matrix through PiC. On the other hand, $\Delta\psi_m$ is increased by an increase in $[P_i]_e$ of less than ~2 mM, but reaches a plateau at $[P_i]_e$ above ~2 mM [16,34,38]. Increases in $\Delta\psi_m$ owing to increases in $[P_i]_e$ is not fully elucidated, but some explanations are proposed. An electroneutral influx of protons ($H^+$) accompanying negatively charged substrates such as $P_i$ does not directly affect $\Delta\psi_m$ but produces a reduction in $\Delta pH$ that promotes proton extrusion by the respiratory chain to maintain $\Delta p$ and eventually increases $\Delta\psi_m$ [35]. Bose et al. [16] provided another explanation: an increase in the influx of $P_i$ activates intramitochondrial NADH production and NADH supply to complex I and also promotes the ability to generate $\Delta p$ by improving the coupling of electron transport between cytochrome *b* and cytochrome *c*, which eventually increases $\Delta\psi_m$. Interestingly, in the present study, ~40 % reduction in the protein level of PiC did not affect glucose-induced hyperpolarization of the mitochondrial inner membrane in spite of a reduction in ATP production. It is possible that the reduction in $P_i$ influx by down-regulation of PiC in the present study is within a range of $P_i$ influx which does not affect $\Delta\psi_m$ as with higher $[P_i]_e$. In addition, our results were derived from sustained down-regulation of $P_i$ influx to mitochondria, as experiments were performed 48 h after transfection of PiC siRNA in contrast with the acute alteration of $P_i$ influx by manipulation of $[P_i]_e$ in previous studies, which may permit adaptation of $\Delta\psi_m$ to maintain $\Delta p$.

It has been generally reported that the contribution of $\Delta\psi_m$ to $\Delta p$ is 80–85 % [34,35,37–45] or more [16] and that of $\Delta pH$ is relatively small, which indicates that the alteration in $\Delta p$ by down-regulation of PiC in the present study is small considering the non-detectable affect on $\Delta\psi_m$. Therefore the supply of $P_i$ to complex V may well be a critical rate-limiting step for ATP production independent of $\Delta p$. The results in the present study demonstrate the critical role of $P_i$ influx to mitochondria in ATP production and metabolism–secretion coupling in pancreatic $\beta$-cells.

## AUTHOR CONTRIBUTION

Yuichi Nishi researched data, contributed to the discussion, wrote the manuscript and revised/edited the manuscript. Shimpei Fujimoto contributed to the discussion, wrote the manuscript and revised/edited the manuscript. Mayumi Sasaki, Eri Mukai, Hiroki Sato, Yuichi Sato, Yumiko Tahara and Yasuhiko Nakamura researched data. Nobuya Inagaki contributed to the discussion and revised/edited the manuscript.

## ACKNOWLEDGEMENTS

We greatly appreciate the gifts of INS-1 cells from Dr Nobuo Sekine (Tokyo Kosei Nenkin Hospital, Tokyo, Japan) and pHMCA5 vector from Dr Hiroyuki Mizuguchi (National Institute of Biomedical Innovation, Ibaraki, Japan). We thank Mr Shinsaku Akagi, Mr Takuro Yamaguchi, Ms Chiyo Kotake and Ms Sara Yasui for technical assistance and Mr Eiji Yoshihara for helpful advice on siRNA transfection.

## FUNDING

This study was supported by a Research Grant on Nanotechnical Medicine from the Ministry of Health, Labour, and Welfare of Japan, Scientific Research Grants, a grant from Innovation Cluster Kansai project of the Ministry of Education, Culture, Sports, Science and Technology of Japan, and a grant from CREST (Core Research for Evolutional Science and Technology) of Japan Science and Technology Cooperation.

## REFERENCES

1 Maechler, P. and Wollheim, C. B. (2001) Mitochondrial function in normal and diabetic $\beta$-cells. Nature **414**, 807–812
2 Kennedy, E. D., Maechler, P. and Wollheim, C. B. (1998) Effects of depletion of mitochondrial DNA in metabolism secretion coupling in INS-1 cells. Diabetes **47**, 374–380
3 Tsuruzoe, K., Araki, E., Furukawa, N., Shirotani, T., Matsumoto, K., Kaneko, K., Motoshima, H., Yoshizato, K., Shirakami, A., Kishikawa, H. et al. (1998) Creation and characterization of a mitochondrial DNA-depleted pancreatic $\beta$-cell line: impaired insulin secretion induced by glucose, leucine, and sulfonylureas. Diabetes **47**, 621–631
4 Palmieri, F. (2004) The mitochondrial transporter family (SLC25): physiological and pathological implications. Pflugers Arch. **447**, 689–709
5 Rubi, B., del Arco, A., Bartley, C., Satrustegui, J. and Maechler, P. (2004) The malate-aspartate NADH shuttle member Aralar1 determines glucose metabolic fate, mitochondrial activity, and insulin secretion in beta cells. J. Biol. Chem. **279**, 55659–55666
6 Casimir, M., Rubi, B., Frigerio, F., Chaffard, G. and Maechler, P. (2009) Silencing of the mitochondrial NADH shuttle component aspartate-glutamate carrier AGC1/Aralar1 in INS-1E cells and rat islets. Biochem. J. **424**, 459–466
7 Chan, C. B., MacDonald, P. E., Saleh, M. C., Johns, D. C., Marban, E. and Wheeler, M. B. (1999) Overexpression of uncoupling protein 2 inhibits glucose-stimulated insulin secretion from rat islets. Diabetes **48**, 1482–1486
8 Zhang, C. Y., Baffy, G., Perret, P., Krauss, S., Peroni, O., Grujic, D., Hagen, T., Vidal-Puig, A. J., Boss, O., Kim, Y. B. et al. (2001) Uncoupling protein-2 negatively regulates insulin secretion and is a major link between obesity, $\beta$ cell dysfunction, and type 2 diabetes. Cell **105**, 745–755
9 Odegaard, M. L., Joseph, J. W., Jensen, M. V., Lu, D., Ilkayeva, O., Ronnebaum, S. M., Becker, T. C. and Newgard, C. B. (2010) The mitochondrial 2-oxoglutarate carrier is part of a metabolic pathway that mediates glucose- and glutamine-stimulated insulin secretion. J. Biol. Chem. **285**, 16530–16537
10 Joseph, J. W., Jensen, M. V., Ilkayeva, O., Palmieri, F., Alarcon, C., Rhodes, C. J. and Newgard, C. B. (2006) The mitochondrial citrate/isocitrate carrier plays a regulatory role in glucose-stimulated insulin secretion. J. Biol. Chem. **281**, 35624–35632
11 Casimir, M., Lasorsa, F. M., Rubi, B., Caille, D., Palmieri, F., Meda, P. and Maechler, P. (2009) Mitochondrial glutamate carrier GC1 as a newly identified player in the control of glucose-stimulated insulin secretion. J. Biol. Chem. **284**, 25004–25014
12 Dolce, V., Iacobazzi, V., Palmieri, F. and Walker, J. E. (1994) The sequences of human and bovine genes of the phosphate carrier from mitochondria contain evidence of alternatively spliced forms. J. Biol. Chem. **269**, 10451–10460
13 Fiermonte, G., Dolce, V. and Palmieri, F. (1998) Expression in *Escherichia coli*, functional characterization, and tissue distribution of isoforms A and B of the phosphate carrier from bovine mitochondria. J. Biol. Chem. **273**, 22782–22787
14 Dolce, V., Fiermonte, G. and Palmieri, F. (1996) Tissue-specific expression of the two isoforms of the mitochondrial phosphate carrier in bovine tissues. FEBS Lett. **399**, 95–98
15 Mayr, J. A., Merkel, O., Kohlwein, S. D., Gebhardt, B. R., Böhles, H., Fötschl, U., Koch, J., Jaksch, M., Lochmüller, H. and Horváth, R. et al. (2007) Mitochondrial phosphate-carrier deficiency: a novel disorder of oxidative phosphorylation. Am. J. Hum. Genet. **80**, 478–484
16 Bose, S., French, S., Evans, F. J., Joubert, F. and Balaban, R. S. (2003) Metabolic network control of oxidative phosphorylation: multiple roles of inorganic phosphate. J. Biol. Chem. **278**, 39155–39165
17 Fujimoto, S., Ishida, H., Kato, S., Okamoto, Y., Tsuji, K., Mizuno, N., Ueda, S., Mukai, E. and Seino, Y. (1998) The novel insulinotropic mechanism of pimobendan: direct enhancement of the exocytotic process of insulin secretory granules by increased $Ca^{2+}$ sensitivity in $\beta$-cells. Endocrinology **139**, 1133–1140
18 Takehiro, M., Fujimoto, S., Shimodahira, M., Shimono, D., Mukai, E., Nabe, K., Radu, R. G., Kominato, R., Aramaki, Y., Seino, Y. and Yamada, Y. (2005) Chronic exposure to $\beta$-hydroxybutyrate inhibits glucose-induced insulin release from pancreatic islets by decreasing NADH contents. Am. J. Physiol. **288**, E372–E380
19 Schultz, V., Sussman, I., Bokvist, K. and Tornheim, K. (1993) Bioluminometric assay of ADP and ATP at high ATP/ADP ratios: assay of ADP after enzymatic removal of ATP. Anal. Biochem. **215**, 302–304
20 Votyakova, T. V. and Reynolds, I. J. (2001) $\Delta\psi_m$-Dependent and -independent production of reactive oxygen species by rat brain mitochondria. J. Neurochem. **79**, 266–277
21 Leung, A. W., Varanyuwatana, P. and Halestrap, A. P. (2008) The mitochondrial phosphate carrier interacts with cyclophilin D and may play a key role in the permeability transition. J. Biol. Chem. **283**, 26312–26323
22 Detimary, P., Gilon, P., Nenquin, M. and Henquin, J. C. (1994) Two sites of glucose control of insulin release with distinct dependence on the energy state in pancreatic B-cells. Biochem. J. **297**, 455–461
23 Detimary, P., Van den Berghe, G. and Henquin, J. C. (1996) Concentration dependence and time course of the effects of glucose on adenine and guanine nucleotides in mouse pancreatic islets. J. Biol. Chem. **271**, 20559–20565
24 Detimary, P., Gilon, P. and Henquin, J. C. (1998) Interplay between cytoplasmic $Ca^{2+}$ and the ATP/ADP ratio: a feedback control mechanism in mouse pancreatic islets. Biochem. J. **333**, 269–274
25 Katz, L. A., Swain, J. A., Portman, M. A. and Balaban, R. S. (1988) Intracellular pH and inorganic phosphate content of heart *in vivo*: a $^{31}$P-NMR study. Am. J. Physiol. **255**, H189–H196
26 Katz, L. A., Swain, J. A., Portman, M. A. and Balaban, R. S. (1989) Relation between phosphate metabolites and oxygen consumption of heart *in vivo*. Am. J. Physiol. **256**, H265–H274
27 Bunger, R., Mallet, R. T. and Hartman, D. A. (1989) Pyruvate-enhanced phosphorylation potential and inotropism in normoxic and postischemic isolated working heart. Near-complete prevention of reperfusion contractile failure. Eur. J. Biochem. **180**, 221–233
28 Ghosh, A., Ronner, P., Cheong, E., Khalid, P. and Matschinsky, F. M. (1991) The role of ATP and free ADP in metabolic coupling during fuel-stimulated insulin release from islet beta-cells in the isolated perfused rat pancreas. J. Biol. Chem. **266**, 22887–22892
29 Erecińska, M., Bryła, J., Michalik, M., Meglasson, M. D. and Nelson, D. (1992) Energy metabolism in islets of Langerhans. Biochim. Biophys. Acta **1101**, 273–295
30 Palmieri, F., Prezioso, G., Quagliariello, E. and Klingenberg, M. (1971) Kinetic study of the dicarboxylate carrier in rat liver mitochondria. Eur. J. Biochem. **22**, 66–74
31 Crompton, M., Palmieri, F., Capano, M. and Quagliariello, E. (1974) The transport of sulphate and sulphite in rat liver mitochondria. Biochem. J. **142**, 127–137
32 Brown, G. C., Lakin-Thomas, P. L. and Brand, M. D. (1990) Control of respiration and oxidative phosphorylation in isolated rat liver cells. Eur. J. Biochem. **192**, 355–362
33 Valdez, L. B., Zaobornyj, T. and Boveris, A. (2006) Mitochondrial metabolic states and membrane potential modulate mtNOS activity. Biochim. Biophys. Acta **1757**, 166–172
34 Dzbek, J. and Korzeniewski, B. (2008) Control over the contribution of the mitochondrial membrane potential ($\Delta\psi$) and proton gradient ($\Delta$pH) to the protonmotive force ($\Delta$p). *In silico* studies. J. Biol. Chem. **283**, 33232–33239
35 Martin, D. B. (1995) Bioenergetics. In A Practical Approach (Brown, G. C. and Cooper, C. E., eds), pp. 39–62, Oxford University Press, Oxford
36 Oliveira, G. A. and Kowaltowski, A. J. (2004) Phosphate increases mitochondrial reactive oxygen species release. Free Radic. Res. **38**, 1113–1118
37 Kunz, W., Gellerich, F. N., Schild, L. and Schönfeld, P. (1988) Kinetic limitations in the overall reaction of mitochondrial oxidative phosphorylation accounting for flux-dependent changes in the apparent $\Delta G^{ex}{}_P/\Delta\mu H^+$ ratio. FEBS Lett. **233**, 17–21
38 Nicholls, D. G. (1974) The influence of respiration and ATP hydrolysis on the proton-electrochemical gradient across the inner membrane of rat-liver mitochondria as determined by ion distribution. Eur. J. Biochem. **50**, 305–315
39 Duszyński, J., Bogucka, K. and Wojtczak, L. (1984) Homeostasis of the protonmotive force in phosphorylating mitochondria. Biochim. Biophys. Acta **767**, 540–547

40 Ouhabi, R., Rigoulet, M., Lavie, J. L. and Guérin, B. (1991) Respiration in non-phosphorylating yeast mitochondria. Roles of non-ohmic proton conductance and intrinsic uncoupling. Biochim. Biophys. Acta **1060**, 293–298
41 Czyż, A., Szewczyk, A., Nałcz, M. J. and Wojtczak, L. (1995) The role of mitochondrial potassium fluxes in controlling the protonmotive force in energized mitochondria. Biochem. Biophys. Res. Commun. **210**, 98–104
42 Rigoulet, M., Fraisse, L., Ouhabi, R., Guerin, B., Fontaine, E. and Leverve, X. (1990) Flux-dependent increase in the stoichiometry of charge translocation by mitochondrial ATPase/ATP synthase induced by almitrine. Biochim. Biophys. Acta **1018**, 91–97
43 Hafner, R. P., Brown, G. C. and Brand, M. D. (1990) Analysis of the control of respiration rate, phosphorylation rate, proton leak rate and protonmotive force in isolated mitochondria using the 'top-down' approach of metabolic control theory. Eur. J. Biochem. **188**, 313–319
44 Lambert, A. J. and Brand, M. D. (2004) Superoxide production by NADH:ubiquinone oxidoreductase (complex I) depends on the pH gradient across the mitochondrial inner membrane. Biochem. J. **382**, 511–517
45 Nobes, C. D., Brown, G. C., Olive, P. N. and Brand, M. D. (1990) Non-ohmic proton conductance of the mitochondrial inner membrane in hepatocytes. J. Biol. Chem. **265**, 12903–12909

Received 19 October 2010/21 January 2011; accepted 25 January 2011
Published as BJ Immediate Publication 25 January 2011, doi:10.1042/BJ20101708

Molecular Genetics and Metabolism 102 (2011) 453–460

Contents lists available at ScienceDirect

Molecular Genetics and Metabolism

journal homepage: www.elsevier.com/locate/ymgme

# *GCKR* mutations in Japanese families with clustered type 2 diabetes

Daisuke Tanaka [a], Kazuaki Nagashima [a], Mayumi Sasaki [a], Chizumi Yamada [a], Shogo Funakoshi [a], Kimiyo Akitomo [a], Katsunobu Takenaka [b], Kouji Harada [c], Akio Koizumi [c], Nobuya Inagaki [a,*]

[a] *Department of Diabetes and Clinical Nutrition, Graduate School of Medicine, Kyoto University, Kyoto, Japan*
[b] *Takayama Red Cross Hospital, Gifu, Japan*
[c] *Department of Health and Environmental Sciences, Graduate School of Medicine, Kyoto University, Kyoto, Japan*

ARTICLE INFO

*Article history:*
Received 15 December 2010
Accepted 15 December 2010
Available online 21 December 2010

*Keywords:*
Genetic susceptibility
Linkage analysis
MODY
*HNF1A*
*GCKR*

ABSTRACT

*Objective:* The aim was to investigate the genetic background of familial clustering of type 2 diabetes.
*Subjects and methods:* We recruited Japanese families with a 3-generation history of diabetes. Genome-wide linkage analysis was performed assuming an autosomal dominant model. Genes in the linkage region were computationally prioritized using Endeavour. We sequenced the candidate genes, and the frequencies of detected nucleotide changes were then examined in normoglycemic controls.
*Results:* To exclude known genetic factors, we sequenced 6 maturity onset diabetes of the young (MODY) genes in 10 familial cases. Because we detected a MODY3 mutation *HNF1A* R583G in one case, we excluded this case from further investigation. Linkage analysis revealed a significant linkage region on 2p25-22 (LOD score = 3.47) for 4 families. The 23.6-Mb linkage region contained 106 genes. Those genes were scored by computational prioritization. Eleven genes, i.e., top 10% of 106 genes, were selected and considered primary candidates. Considering their functions, we eliminated 3 well characterized genes and finally sequenced 8 genes. *GCKR* ranked highly in the computational prioritization. Mutations (minor allele frequency less than 1%) in exons and the promoter of *GCKR* were found in index cases of the families (3 of 18 alleles) more frequently than in controls (0 of 36 alleles, P = 0.033). In one pedigree with 9 affected members, the mutation *GCKR* g.6859C>G was concordant with affection status. No mutation in other 7 genes that ranked highly in the prioritization was concordant with affection status in families.
*Conclusions:* We propose that *GCKR* is a susceptibility gene in Japanese families with clustered diabetes. The family based approach seems to be complementary with a large population study.


## 1. Introduction

The national survey in 2007 reported that 8.9 million people suffer from diabetes in Japan [1]. Most of these have type 2 diabetes, and the number of such patients has increased continuously. Both genetic and environmental factors play important roles in the pathogenesis of type 2 diabetes [2].

To elucidate the genetic factors underlying the pathogenesis of type 2 diabetes in the Japanese population, several genome-wide linkage analyses in Japanese sib-pairs have been performed [3–5]. Linkage to 11p13–p12 is consistently implicated in these studies [5]. Recent successes with genome-wide association analyses in the Japanese population have revealed a susceptibility variant in *KCNQ1* located at 11p15.5 [6,7], a locus not far from the region suggested in linkage analyses. The association of susceptibility loci including *TCF7L2*, *CDKAL1*, *CDKN2A/B*, *IGF2BP2*, *SLC30A8*, and *HHEX* with diabetes has been established in Caucasian populations and replicated in the Japanese population [8]. However, the loci identified in association studies have uniformly small effect sizes, and can explain only a small portion of the genetic background of diabetes in the Japanese population. Approaches other than sib-pair linkage analyses and association analyses may therefore be required to elucidate a greater aspect of the genetic background of type 2 diabetes.

In the present study, we used a family-based approach, because high degrees of familial clustering can raise the relative risk and provide better insight to novel loci of larger effect size [9]. Familial clustering of diabetes is well known, the typical example being MODY [10]. On the other hand, in most families in Japan, familial clustering cannot be attributed to mutations of the 6 known MODY genes [10], and genetic predisposition in such families has not been ascertained.

We recruited families having a 3-generation history of diabetes and performed genome-wide linkage analysis. We selected candidate genes in the linked chromosomal region and searched for rare and

*Abbreviations:* GAD, glutamic acid decarboxylase; GCKR, glucokinase regulator; HLOD, heterogeneity logarithm of the odds; HNF4α, Hepatocyte Nuclear Factor 4α; LOD, logarithm of the odds; MAF, minor allele frequency; MODY, maturity onset diabetes of the young; RFLP, restriction fragment length polymorphism; SNP, single nucleotide polymorphism.

* Corresponding author. Department of Diabetes and Clinical Nutrition, Graduate School of Medicine, Kyoto University, 54 Shogoin-Kawahara-cho, Sakyo-ku, Kyoto, 606-8507, Japan. Fax: +81 75 771 6601.
*E-mail address:* inagaki@metab.kuhp.kyoto-u.ac.jp (N. Inagaki).

1096-7192/$ – see front matter © 2010 Elsevier Inc. All rights reserved.
doi:10.1016/j.ymgme.2010.12.009

common nucleotide changes in the genes in familial cases and unaffected controls.

## 2. Material and methods

### 2.1. Families and additional index cases

We recruited patients from collaborating hospitals in Japan who had diabetes with a 3-generation family history, which is suggestive of autosomal dominant mode of inheritance [11]. If ≥2 family members with diabetes were alive and donated DNA, the families were regarded as suitable subjects for the present study. Families including members with positive GAD (glutamic acid decarboxylase) antibody were excluded from the study. Four families met these criteria and were included in the linkage analysis (Fig. 1). Affected status of the participants was determined in two ways. First, if participants had been diagnosed with diabetes and treated with oral hypoglycemic agents or insulin injection, they were regarded as affected. Second, if participants had not been treated with oral hypoglycemic agents or insulin injection, they underwent HbA1c (Hemoglobin $A_{1c}$) measurement for screening of impaired glucose tolerance. The value for HbA1c is estimated as an NGSP (US National Glycohemoglobin Standardization Program) equivalent value (%) calculated by the formula HbA1c (%) = HbA1c (JDS, Japanese Diabetes Society) (%) + 0.4%, considering the relational expression of HbA1c (JDS)(%) measured by the previous Japanese standard substance and measurement methods and HbA1c (NGSP) [12]. If their HbA1c levels were ≥6.0%, they were also regarded as affected. HbA1c ≥6.0% is the level defined as possible diabetes mellitus in the 2007 survey of the Ministry of Labor, Health and Welfare of Japan [1]. In addition to these subjects, 6 index cases from other families with a 3-generation history of diabetes were included in the study (Supplementary Fig. 1). In these families, although we confirmed the affected status of some of the family members, DNA samples were available only for the index cases but not for other family members. Together with the 4 index cases from the families included in the linkage analysis, a total of 10 unrelated cases with a 3-generation history of diabetes were available for DNA sequencing. The clinical features of family members and additional index cases are shown in Table 1.

### 2.2. Normoglycemic controls

An annual medical check-up program was performed in Nyukawa district of Takayama City, Japan. Nine-hundred ninety local residents (430 men, 560 women) were recruited in the program and consented to donate their DNA. From 2002 to 2007, participants underwent physical examination and blood tests including fasting plasma glucose and HbA1c every year. We selected normoglycemic controls from the

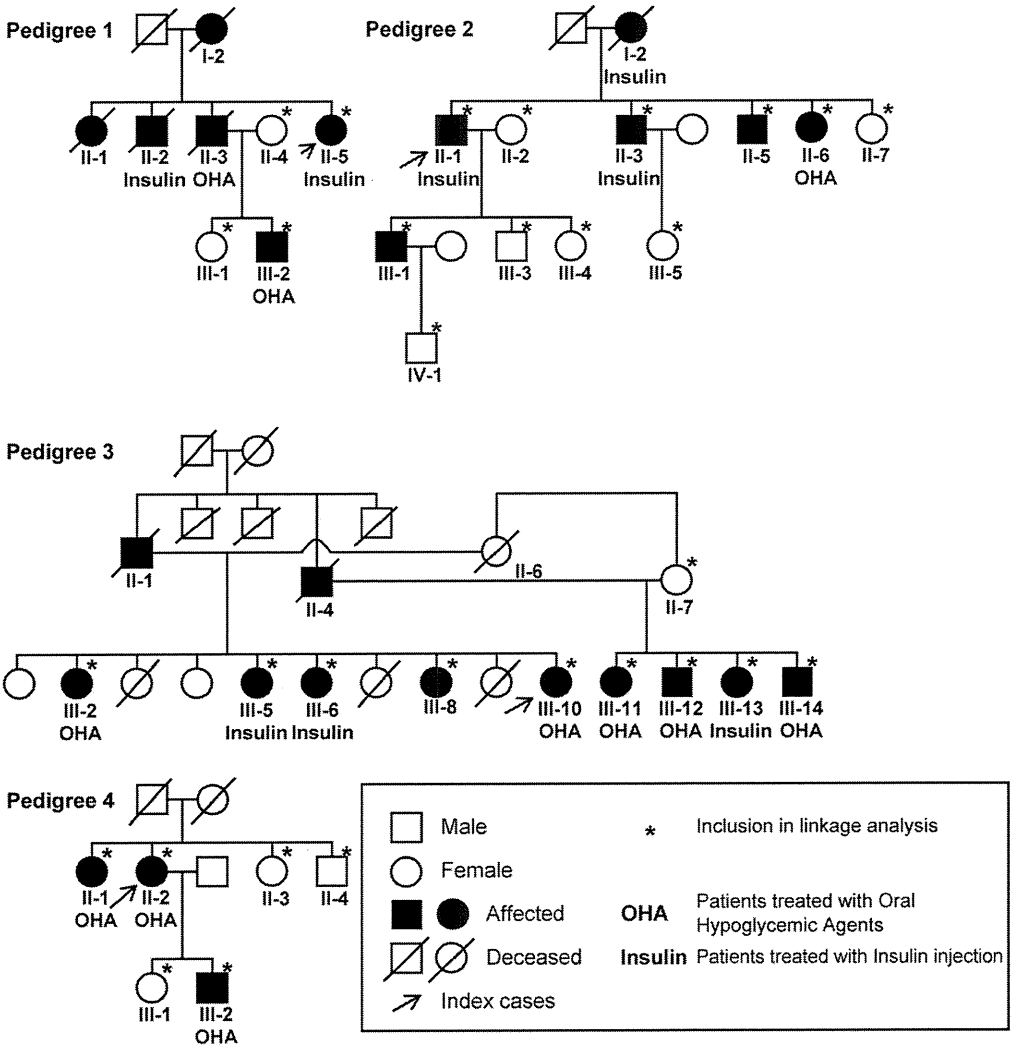


**Fig. 1.** Four pedigrees with familial aggregated diabetes mellitus.

**Table 1**
Characteristics of family members and additional index cases.

| | ID | Current age | Sex | BMI | HbA1c (%) | Age when diagnosed (diagnosis) | Current therapy |
|---|---|---|---|---|---|---|---|
| Pedigree 1 | II-4 | 70 | F | 16.2 | 5.0 | | |
| | II-5 | 71 | F | 22.5 | 10.6 | 60 (DM) | Insulin 66 U/d |
| | III-1 | 40 | F | 21.9 | 5.4 | | |
| | III-2 | 37 | M | 26.0 | 6.9 | 20 (DM) | Insulin |
| Pedigree 2 | II-1 | 79 | M | 19.2 | 7.5 | 50 (DM) | Insulin 25 U/d |
| | II-2 | 77 | F | 18.6 | 5.6 | | |
| | II-3 | 76 | M | 17.9 | 7.2 | 45 (DM) | Insulin |
| | II-5 | 74 | M | 18.2 | 6.0 | 64 (IGT) | Diet |
| | II-6 | 71 | F | 18.4 | 6.6 | N/A (DM) | Oral drug |
| | II-7 | 68 | F | 19.9 | 5.9 | | |
| | III-1 | 53 | M | 24.2 | 6.0 | 53 (IGT) | Diet |
| | III-3 | 51 | M | 20.4 | 5.6 | | |
| | III-4 | 47 | F | 19.3 | 5.2 | | |
| | III-5 | 46 | F | 19.6 | 4.9 | | |
| | IV-1 | 23 | M | 19.9 | 5.6 | | |
| Pedigree 3 | II-7 | 92 | F | 22.3 | 5.9 | | |
| | III-2 | 77 | F | 23.9 | 9.3 | 30 (DM) | Oral drug |
| | III-5 | 72 | F | 22.0 | 8.1 | 60 (DM) | Insulin 16 U/d |
| | III-6 | 69 | F | 19.8 | 8.0 | 65 (DM) | Insulin 16 U/d |
| | III-8 | 66 | F | 19.1 | 6.5 | 64 (IGT) | Diet |
| | III-10 | 59 | F | 19.3 | 10.2 | 57 (DM) | Oral drug |
| | III-11 | 67 | F | 20.4 | 6.9 | 62 (DM) | Oral drug |
| | III-12 | 66 | M | 21.1 | N/A | 57 (DM) | Oral drug |
| | III-13 | 64 | F | 20.0 | 6.6 | 25 (DM) | Insulin |
| | III-14 | 62 | M | 20.2 | 10.3 | 50 (DM) | Oral drug |
| Pedigree 4 | II-1 | 76 | F | 28.2 | 6.7 | 60 (DM) | Oral drug |
| | II-2 | 73 | F | 25.1 | 6.4 | 50 (DM) | Oral drug |
| | II-3 | 67 | F | 19.0 | 5.5 | | |
| | II-4 | 64 | M | N/A | 5.4 | | |
| | III-1 | 52 | F | 20.4 | 5.3 | | |
| | III-2 | 50 | M | 20.8 | 6.2 | 35 (DM) | Oral drug |
| Additional index cases | 1 | 57 | M | 25.7 | 7.1 | 30 (DM) | Oral drug |
| | 2 | 47 | F | 22.9 | 10.0 | 36 (DM) | Insulin 20 U/d |
| | 3 | 68 | F | 19.7 | 7.1 | 45 (DM) | Insulin 19 U/d |
| | 4 | 60 | F | 24.7 | 10.4 | 40 (DM) | Insulin 51 U/d |
| | 5 | 60 | F | 28.0 | 9.7 | 50 (DM) | Insulin 8 U/d |
| | 6 | 54 | F | 34.5 | 9.1 | 40 (DM) | Insulin |

BMI: body mass index, DM: diabetes mellitus, IGT: impaired glucose tolerance.

participants in the cohort. Subjects defined as normoglycemic controls had the following characteristics: HbA1c <6.0% and fasting plasma glucose <5.5 mmol/l during 5-year follow-up span, and age ≥55. The number of subjects that satisfied the definition was 206 (81 men, 125 women).

### 2.3. Genotyping family members

Genomic DNA was extracted from blood samples with a QIAamp DNA Blood Mini Kit (Qiagen Inc). PCR amplification from genomic DNA was performed with fluorescence-labeled (6-FAM, HEX, NED) and tailed primers. PCR primers to analyze microsatellite markers comprised an approximately 10 cM human index map (ABI Prism Linkage Mapping Set Version 2.5: 382 markers for 22 autosomes), and other microsatellite fine markers were designed according to information from the UniSTS map. PCR reactions were carried out in 7.5 μl with 50 ng genomic DNA, using AmpliTaq Gold DNA Polymerase (Applied Biosystems) in a 2-step amplification program. DNA fragments were analyzed on an Applied Biosystems 3130 Genetic Analyzer. Genotyping errors and inconsistent relationships were checked with the use of GENEHUNTER (version 2.1) software [13]. If the results of genotyping were missed or ambiguous, we treated them as an unknown genotype in the linkage analysis. The rate of genotyping failure was 0.057% (7/11842).

### 2.4. Linkage and haplotype analyses

Both affected and unaffected family members were included in the linkage analysis. Participants with HbA1c level <6.0% were considered unaffected if the age was ≥55 and unknown if the age was <55, considering the assumed age-dependent penetrance of diabetes. The purpose of including members assigned as unknown was to increase the accuracy of haplotype estimation in affected members, although inclusion did not increase the statistical power. Multipoint parametric analyses for autosomes were run using GENEHUNTER assuming an autosomal dominant model [13]. Because locus heterogeneity could be associated with diabetes, LOD (log of the odds) score and HLOD (heterogeneity LOD) score were calculated. The disease allele frequency was set at 0.00001 and a phenocopy frequency of 0.00001 was assumed. Population allele frequencies for each microsatellite marker were assigned equal portions for individual alleles. We used a 2-stage design: first, all chromosomal regions were screened by genotyping at an approximately 10 cM density (screening), and the regions where LOD scores were highest were considered potentially interesting. Second, these regions were further finely mapped at approximately 1- to 2-cM densities (fine mapping). Regions where LOD scores were above 3.3, a level corresponding to genome-wide significance [9], were considered linkage regions. Haplotypes were constructed with the GENEHUNTER program.

### 2.5. Prioritization of candidate genes

The 23.6-Mb linkage region on chromosome 2p25-22 contained 106 genes annotated in Ensemble genome browser (http://www.ensembl.org). The genes were computationally prioritized using Endeavour (http://www.esat.kuleuven.be/endeavour/) [14]. We selected 6 MODY genes (*HNF4A*, *GCK*, *HNF1A*, *PDX1*, *HNF1B*, and *NEUROD1*) as training genes because a dominant mode of inheritance

was assumed in the highly clustered families in linkage analysis. We adopted all databases available in Endeavour, which prioritized glucokinase regulator (*GCKR*) at the first rank.

### 2.6. Sequencing

We directly sequenced the coding exons of 6 MODY genes (*HNF4A*, *GCK*, *HNF1A*, *PDX1*, *HNF1B*, and *NEUROD1*) in the 10 index cases. We sequenced *GCKR* including all exons found in the National Center for Biotechnology Information (NCBI) Evidence Viewer (http://www.ncbi.nlm.nih.gov) and the 2-kb promoter region in the index cases from families and in control subjects. We also selected other 7 genes that are highly prioritized within the 11th rank (10.3%) in the linkage region using Endeavour excluding 3 genes with known metabolic functions unrelated to glucose metabolism (Supplementary Table 1). We sequenced the entire coding exons of the 7 genes in the index cases from families included in the linkage analysis. Forward and reverse PCR primers for each exon were selected in an intronic sequence 50 bp away from the intron/exon boundaries and primers to amplify the *GCKR* promoter region were also selected. Sequencing primer data for *GCKR* is shown in Supplementary Table 2. PCR products were run on 2% agarose gel, and the appropriate bands were excised and then purified with the use of the QIAquick Gel Extraction Kit (Qiagen). Sequencing results were analyzed on an ABI Prism 3130 Avant DNA sequencer (Applied Biosystems). Any nucleotide changes identified in sequencing were searched for SNPs (single nucleotide polymorphisms) in the dbSNP database (http://www.ncbi.nlm.nih.gov/SNP/).

### 2.7. Genotyping SNPs

If minor allele frequencies (MAF) of nucleotide changes identified in sequencing were unregistered in the HapMap JPT database on dbSNP as of April 2010 and the minor allele appeared in <2 of all subjects, MAF was determined in the expanded population. We defined mutation as MAF <1% [15]. To determine whether each nucleotide change was a mutation or not, we genotyped 105 normoglycemic controls randomly selected from the cohort (Supplementary Table 3), because genotyping of 210 normal chromosomes is necessary to achieve 80% power to detect a polymorphism present in 1% of the population [16]. The PCR-RFLP (restriction fragment length polymorphism) method for *HNF1A* R583G, *GCKR* g.-689G>A, *GCKR* g.-299G>A, *GCKR* E252K and *FOSL2* R198H and Taqman method for *GCKR* g.6859C>G were used.

### 2.8. Statistical analysis

Frequencies of mutations (MAF<1%) and common nucleotide changes (MAF≥1%) identified in *GCKR* sequencing in the index cases and in normoglycemic controls were compared by the Fisher exact test with SAS software (version 8.2).

### 2.9. Ethics

The methods used in this study were approved by the Ethics Committee of the Kyoto University Institutional Review Board, and approved written informed consent was obtained from each participant.

## 3. Results

### 3.1. Characteristics of family members

Four families with a 3-generation history of diabetes were enrolled in this study (Fig. 1, Table 1). Every family included no less than 1 member that had been diagnosed with diabetes before the age of 50. Sixteen members (6 men, 10 women) had previously been diagnosed with diabetes. Thirteen out of the 16 members with diabetes were lean (BMI<25). Six members were treated with insulin and another 10 members were treated with oral hypoglycemic agents. Twelve family members who had not been diagnosed with diabetes underwent HbA1c measurement and 3 of them had HbA1c level ≥6.0%. These 3 members had already been diagnosed with impaired glucose tolerance before this study and were included as affected members in the study.

### 3.2. Exclusion of MODY gene mutations in the index cases

For the 10 index cases, we performed direct sequencing in entire coding exons of the MODY genes. The detected missense SNPs were *HNF1A* I27L (rs1169288), *HNF1A* S487N (rs2464196), *HNF1A* R583G, and *HNF4A* T117I (rs1800961) (Supplementary Table 4). *HNF1A* R583G is a mutation that is reported to cause MODY [17], thus we excluded the carrier of the mutation (additional index case #6, Table 1) from further investigation. *HNF1A* I27L and *HNF1A* S487N are common in the general population (MAF=0.386 and 0.341, respectively in HapMap-JPT). *HNF4A* T117I was associated with late-onset type 2 diabetes but it was not the cause of MODY in a previous report [18].

### 3.3. Linkage analysis

A total of 30 members (19 affected members) from 4 families were included in the linkage analysis, assuming an autosomal dominant model. The genome-wide linkage results in the screening are shown in Fig. 2. Regions of potential interest by multipoint LOD and HLOD scores were observed on chromosomes 2p24 and 7q34. After fine mapping, 2p25-22 was revealed to be a significant linkage region (Fig. 3, LOD and HLOD=3.47) while the region on 7q34 was discarded. The size of the region with positive HLOD score was 23.6 Mb (D2S2199–D2S2230). In the region, a haplotype segregated in affected and unaffected members in the pedigrees 1, 2, and 3, but not in the pedigree 4.

### 3.4. Candidate genes

We searched candidate genes in the implicated linkage region by applying a gene prioritization approach implemented in Endeavour software. We selected 6 MODY genes as training genes. The 2 top-ranked genes were glucokinase regulatory protein (*GCKR*) and nuclear receptor coactivator 1 (*NCOA1*). *GCKR* ranked high in prioritization using gene–gene interaction databases (first rank in 5 out of 7 interaction databases), mainly because the interaction of glucokinase and glucokinase regulatory protein has been demonstrated in previous studies [19,20]. *NCOA1* also ranked high in prioritization using gene–gene interaction databases (second rank in 2 out of 7 interaction databases), because nuclear receptor coactivator 1 has been reported to interact with HNF4α (Hepatocyte Nuclear Factor 4α) as a coactivator [21]. Together with *GCKR* and *NCOA1*, genes that are highly prioritized within the 11th rank (10.3% of annotated genes) were considered candidate genes except 3 genes with well-characterized metabolic functions unrelated to glucose metabolism (Supplementary Table 1).


**Fig. 2.** Multipoint HLOD and LOD scores in genome-wide linkage analysis for 4 pedigrees.

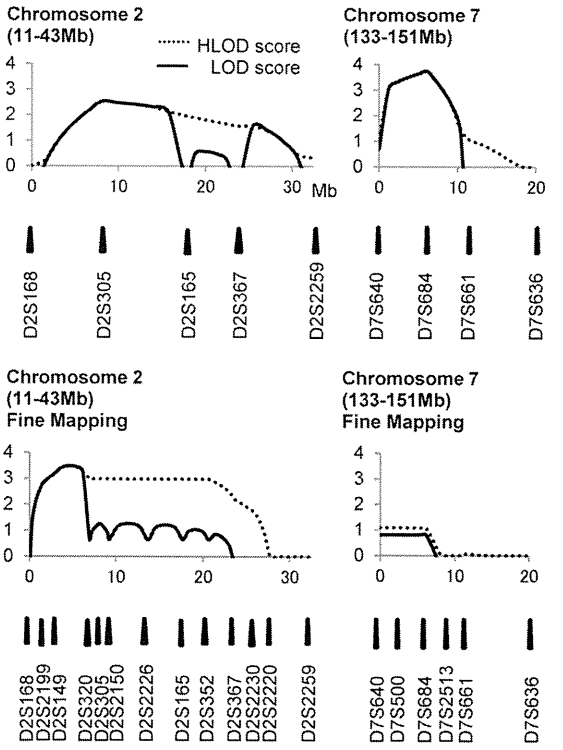


**Fig. 3.** Multipoint HLOD and LOD scores in fine mapping of D2S168–D2S2259 and D7S640–D7S636.

### 3.5. Direct sequencing in GCKR and other candidate genes

We performed direct sequencing in exons and the 2-kb promoter region of *GCKR*. Sequencing was performed in 9 index cases from families and in 18 normoglycemic controls in parallel. The 18 control subjects were randomly selected from 206 normoglycemic controls (Supplementary Table 3). Detected sequence changes in the 9 index cases and 18 controls are shown in Table 2. Five nucleotide changes (g.-959 Insertion AATGTTG, E66E, E77G, g.9709G>A, and L446P) were considered to be common variants, because the minor allele was found in not less than 2 subjects out of a total of 27 case and control subjects. To determine whether or not each of the other nucleotide changes (g.-689G>A, g.-299G>A, E252K and g.6859C>G) was a mutation (MAF<1%), genotyping was performed in a total of 105 normoglycemic controls. g.-689G>A, g.-299G>A and g.6859C>G were not detected in the 105 controls, and were regarded as mutations, while E252K was detected in 4 controls out of 105 (MAF = 1.9%) and was regarded as a common change. The number of alleles having mutations was thus significantly larger in the index cases from families than in the controls (3/18 alleles vs. 0/36 alleles, P = 0.033, Fisher exact test).

We performed direct sequencing in the entire coding exons of other 7 candidate genes in index cases from 4 families. One misssense mutation *FOSL2* R198H (MAF = 0.004 in normoglycemic controls) was detected. No other mutations were detected in other 6 genes (Supplementary Table 5).

### 3.6. Segregation of the mutations with the phenotype in pedigrees

In index cases from the 4 families included in the linkage analysis, 3 sequence changes of *GCKR* were detected (g.-959 Insertion AATGTTG, g.6859C>G and L446P). We tested the segregation of *GCKR* g.6859C>G, a mutation detected in pedigree 3, with the phenotype in the pedigree. Another 2 changes (*GCKR* g.-959 Insertion AATGTG and *GCKR* L446P) were commonly detected in controls (3/36 alleles and 11/36 alleles respectively). In pedigree 3, *GCKR* g.6859C>G was detected in all 9 affected members, but was not detected in the unaffected member (II-7). We performed linkage analysis and haplotype construction in 2p25-22 using the *GCKR* g.6859 genotype together with the microsatellite markers. The parametric multipoint LOD score for pedigree 3 was 2.67 at the *GCKR* g.6859 locus. Haplotype analysis revealed that all affected individuals in pedigree 3 shared a disease haplotype within D2S2199–D2S2230, which includes *GCKR* g.6859G (Fig. 4). In pedigree 3, another sequence change, *GCKR* L446P, was detected, but *GCKR* L446P did not co-segregate with the disease. Haplotype analysis revealed that the minor allele of *GCKR* L446P (g.11169C) resided on a different haplotype than *GCKR* g.6859G in affected subjects III-11, 12, 13, 14 (Fig. 4).

We tested the segregation of *FOSL2* R198H, a mutation detected in pedigree 4, with the phenotype. *FOSL2* R198H was detected in 2 affected subjects (II-2, II-22) but not detected in one subject (II-1).

## 4. Discussion and conclusions

Recent progress in genome-wide association studies has identified tens of type 2 diabetes susceptibility genes. Even so, only a small

**Table 2**
Mutations and common nucleotide changes in exons and the promoter of *GCKR* in 9 index cases in families and in 18 controls.

| Position | Change | Description | Effect | Detected number of alleles | | | | $p^a$ | Minor allele frequency [MAF] |
|---|---|---|---|---|---|---|---|---|---|
| | | | | Index cases from families (n = 9) | | Controls (n = 18) | | | |
| | | | | Major | Minor | Major | Minor | | |
| Mutations (MAF<1%) | | | | | | | | | |
| Promoter | g.-689G>A | | | 17 | 1 | 36 | 0 | 0.33 | 0.000[b] |
| Promoter | g.-299G>A | | | 17 | 1 | 36 | 0 | 0.33 | 0.000[b] |
| Exon 9 | g.6859C>G | Noncoding exon | | 17 | 1 | 36 | 0 | 0.33 | 0.000[b] |
| Total | | | | 15 | 3 | 36 | 0 | 0.033 | |
| Common changes | | | | | | | | | |
| Promoter | g.-959 insAATGTTG | | | 16 | 2 | 33 | 3 | 1.00 | N/D |
| Exon 2 | g.468G>A | Synonymous | E66E | 17 | 1 | 35 | 1 | 1.00 | N/D |
| Exon 3 | g.671A>G | Missense | E77G | 17 | 1 | 33 | 3 | 1.00 | 0.024[c] |
| Exon 10 | g.8817G>A | Missense | E252K | 18 | 0 | 35 | 1 | 1.00 | 0.019[b] |
| Exon 11 | g.9709G>A | Noncoding exon | | 17 | 1 | 33 | 3 | 1.00 | 0.123[c] |
| Exon 14 | g.11169T>C | Missense | L446P | 8 | 10 | 25 | 11 | 0.087 | 0.467[c] |

GenBank accession no. NT_022184.15.
[a] Fisher exact test.
[b] Frequency in 105 normoglycemic controls.
[c] Frequency in HapMap-JPT.

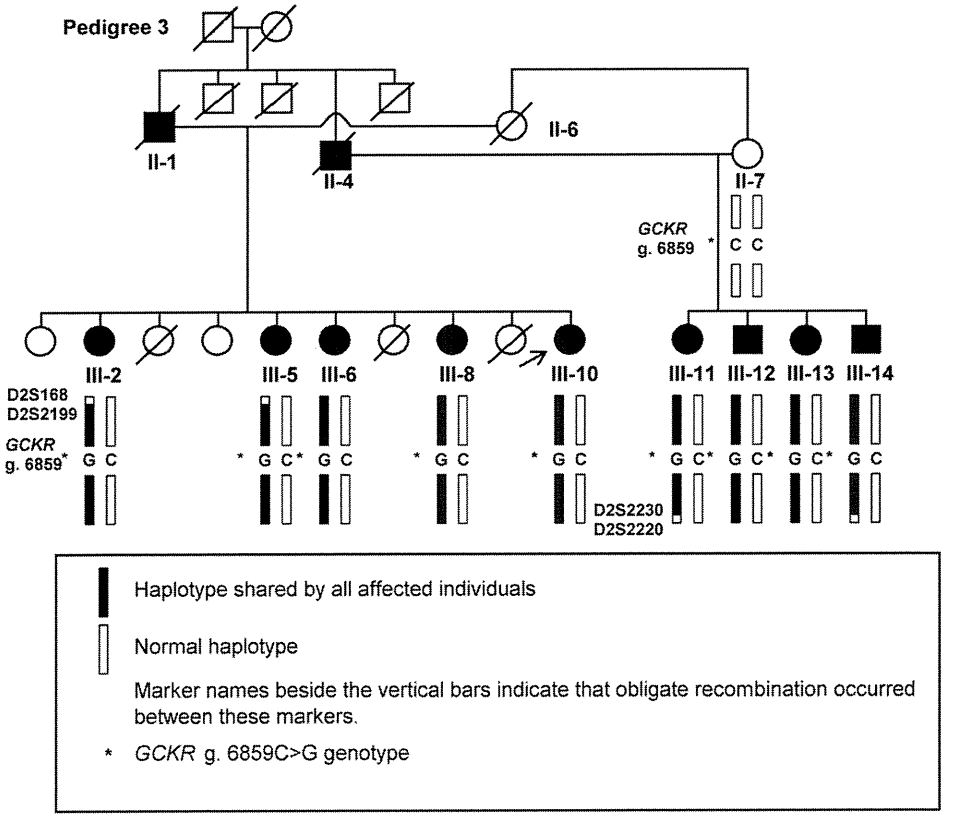


**Fig. 4.** Haplotype analysis in the D2S168–D2S2259 region and the *GCKR* g.6859C>G genotype for pedigree 3.

portion of the genetic background of diabetes has been explained in the Japanese population. The loci identified in association studies have only very small effect sizes. We hypothesized that rare disease variants with larger effect sizes remain to be discovered that may explain a greater part of the genetic background. Family-based linkage study is an important alternative for the identification of rare disease variants. Indeed, studies with large families with highly clustered diabetes have revealed important mutations involved in MODY and other dominantly inherited diabetes, including a *KCNJ11* mutation [22]. We therefore recruited families with a 3-generation history of diabetes. The validity of our strategy was strengthened by the fact that one case out of the 10 index cases recruited in our study carried a previously reported rare disease variant *HNF1A* R583G.

Our family analysis revealed a significant linkage region on chromosome 2p25-22 that has not been reported in previous Japanese sib-pair analyses [3–5]. Because our approach was based on a higher degree of familial clustering than sib-pair analyses, the linkage region suggested in the present study might well go undetected in sib-pair analyses that include an admixture of sib-pairs with both low and high degrees of familial clustering. In the present study, we conducted a computational approach targeting the linkage region on chromosome 2p25-22. One hundred and six known genes were present in this linkage region. Prioritization of the candidate gene was possible by integrating the information available from multiple publicly available databases [14]. *GCKR* and other 7 gens ranked high in the prioritization, and were selected as candidate genes.

GCKR regulates glucokinase (GCK), the first glycolytic enzyme, in liver. *GCKR*-null mice exhibit elevated postprandial glucose [19]. Adenoviral-mediated overexpression of *GCKR* in mouse liver increases GCK activity and lowers fasting blood glucose. It was suggested that GCKR, a competitive inhibitor of GCK activity, also has a paradoxical role in extending GCK half-life by stabilizing the enzyme [20]. If so, diminished expression of GCKR in human might cause decreased GCK activity in liver and lead to impaired liver glucose uptake, which suggests the *GCKR* mutation as a possible cause of the disease in linked families.

We sequenced entire exons and the 2-kb promoter region of *GCKR* in 9 index 3-generation cases and in 18 control subjects. The rare variants were significantly more frequent in index cases from families than in control subjects. In addition, exonic rare variant g.6859C>G in pedigree 3, which was not detected in 105 control subjects, was clearly segregated in all 9 affected members in pedigree 3. Previous reports have shown the association of common *GCKR* variants with fasting plasma glucose, glucose level after glucose challenge, and diabetes risk in various ethnic groups [23–30]. In Japanese population, a common variant *GCKR* rs780094 is associated with fasting glucose and diabetes risk [27,30]. Our family study suggests the effect of rare *GCKR* variants on diabetes susceptibility that has not been revealed by previous association studies. A recent study has shown the excess of rare *GCKR* variants in individuals with hypertriglyceridemia [31], which supports our idea that rare *GCKR* mutations also affect the diabetes susceptibility.

On the other hand, the only one mutation in other 7 highly prioritized genes was *FOSL2* R198H and it did not co-segregate with the phenotype in the pedigree. Therefore, we tentatively eliminate the possibility that these genes are involved in familial clustering of diabetes patients in the current pedigrees.

Our study has several limitations. First is the large size (23.6 Mb) of the linkage region. Only 4 families could be included in the linkage analysis because we limited the cohort to 3-generation families with $\geq 2$ affected members who donated DNA. Further efforts to recruit large families are needed to narrow down the linkage region. Second, because the *GCKR* g.6859C>G mutation was in a non-coding exon, confirming the relevance of the mutation as the cause of the disease is difficult. Investigation of the effect of the mutation in human liver, where GCKR is predominantly expressed [32], is required, but liver specimens of family

members are currently unavailable. Although we tried to determine the mRNA level in peripheral blood of family members, GCKR mRNA was only barely detectable with the RT-PCR method (data not shown), so comparison of the GCKR mRNA level between affected and unaffected members was not possible. We speculate that the g.6859C>G mutation might affect GCKR function in liver through mRNA transcription or splicing processes [33]. *GCKR* g.-689G>A and g.-299G>A mutations located in the promoter also might affect the expression of GCKR, but TRANSFAC database [34] expected no binding sites of transcription factors at the two promoter mutations.

In conclusion, with systematic investigation we propose that *GCKR* is a susceptibility gene in Japanese families with clustered diabetes. A family-based approach may be a promising strategy to elucidate the complex genetic background of common diseases including type 2 diabetes.

Supplementary materials related to this article can be found online at doi:10.1016/j.ymgme.2010.12.009.

## Acknowledgments

This work was supported by a grant for Research on Human Genome Tailor-Made from the Ministry of Health, Labor, and Welfare of Japan, a grant for Intractable Disease Research Program from the Ministry of Health, Labor, and Welfare of Japan, Scientific Research Grants from the Ministry of Education, Culture, Sports, Science, and Technology of Japan, and a grant from Core Research for Evolutional Science and Technology (CREST) of Japan Science and Technology Cooperation, and by Kyoto University Global COE Program "Center for Frontier Medicine".

## References

[1] Ministry of Health, Labor and Welfare of Japan, Health and Nutrition Survey. 2007, 2008.
[2] S. O'Rahilly, I. Barroso, N.J. Wareham, Genetic factors in type 2 diabetes: the end of the beginning? Science 307 (2005) 370–373.
[3] Y. Mori, S. Otabe, C. Dina, K. Yasuda, C. Populaire, C. Lecoeur, V. Vatin, E. Durand, K. Hara, T. Okada, K. Tobe, P. Boutin, T. Kadowaki, P. Froguel, Genome-wide search for type 2 diabetes in Japanese affected sib-pairs confirms susceptibility genes on 3q, 15q, and 20q and identifies two new candidate loci on 7p and 11p, Diabetes 51 (2002) 1247–1255.
[4] N. Iwasaki, N.J. Cox, Y.Q. Wang, P.E. Schwarz, G.I. Bell, M. Honda, M. Imura, M. Ogata, M. Saito, N. Kamatani, Y. Iwamoto, Mapping genes influencing type 2 diabetes risk and BMI in Japanese subjects, Diabetes 52 (2003) 209–213.
[5] H. Nawata, S. Shirasawa, N. Nakashima, E. Araki, J. Hashiguchi, S. Miyake, T. Yamauchi, K. Hamaguchi, H. Yoshimatsu, H. Takeda, H. Fukushima, T. Sasahara, K. Yamaguchi, N. Sonoda, T. Sonoda, M. Matsumoto, Y. Tanaka, H. Sugimoto, H. Tsubouchi, T. Inoguchi, T. Yanase, N. Wake, K. Narazaki, T. Eto, F. Umeda, M. Nakazaki, J. Ono, T. Asano, Y. Ito, S. Akazawa, I. Hazegawa, N. Takasu, M. Shinohara, T. Nishikawa, S. Nagafuchi, T. Okeda, K. Eguchi, M. Iwase, M. Ishikawa, M. Aoki, N. Keicho, N. Kato, K. Yasuda, K. Yamamoto, T. Sasazuki, Genome-wide linkage analysis of type 2 diabetes mellitus reconfirms the susceptibility locus on 11p13–p12 in Japanese, J. Hum. Genet. 49 (2004) 629–634.
[6] K. Yasuda, K. Miyake, Y. Horikawa, K. Hara, H. Osawa, H. Furuta, Y. Hirota, H. Mori, A. Jonsson, Y. Sato, K. Yamagata, Y. Hinokio, H.Y. Wang, T. Tanahashi, N. Nakamura, Y. Oka, N. Iwasaki, Y. Iwamoto, Y. Yamada, Y. Seino, H. Maegawa, A. Kashiwagi, J. Takeda, E. Maeda, H.D. Shin, Y.M. Cho, K.S. Park, H.K. Lee, M.C. Ng, R.C. Ma, W.Y. So, J.C. Chan, V. Lyssenko, T. Tuomi, P. Nilsson, L. Groop, N. Kamatani, A. Sekine, Y. Nakamura, K. Yamamoto, T. Yoshida, K. Tokunaga, M. Itakura, H. Makino, K. Nanjo, T. Kadowaki, M. Kasuga, Variants in KCNQ1 are associated with susceptibility to type 2 diabetes mellitus, Nat. Genet. 40 (2008) 1092–1097.
[7] H. Unoki, A. Takahashi, T. Kawaguchi, K. Hara, M. Horikoshi, G. Andersen, D.P. Ng, J. Holmkvist, K. Borch-Johnsen, T. Jorgensen, A. Sandbaek, T. Lauritzen, T. Hansen, S. Nurbaya, T. Tsunoda, M. Kubo, T. Babazono, H. Hirose, M. Hayashi, Y. Iwamoto, A. Kashiwagi, K. Kaku, R. Kawamori, E.S. Tai, O. Pedersen, N. Kamatani, T. Kadowaki, R. Kikkawa, Y. Nakamura, S. Maeda, SNPs in KCNQ1 are associated with susceptibility to type 2 diabetes in East Asian and European populations, Nat. Genet. 40 (2008) 1098–1102.
[8] K. Miyake, W. Yang, K. Hara, K. Yasuda, Y. Horikawa, H. Osawa, H. Furuta, M.C. Ng, Y. Hirota, H. Mori, K. Ido, K. Yamagata, Y. Hinokio, Y. Oka, N. Iwasaki, Y. Iwamoto, Y. Yamada, Y. Seino, H. Maegawa, A. Kashiwagi, H.Y. Wang, T. Tanahashi, N. Nakamura, J. Takeda, E. Maeda, K. Yamamoto, K. Tokunaga, R.C. Ma, W.Y. So, J.C. Chan, N. Kamatani, H. Makino, K. Nanjo, T. Kadowaki, M. Kasuga, Construction of a prediction model for type 2 diabetes mellitus in the Japanese population based on 11 genes with strong evidence of the association, J. Hum. Genet. 54 (2009) 236–241.
[9] E.S. Lander, N.J. Schork, Genetic dissection of complex traits, Science 265 (1994) 2037–2048.
[10] K. Yamagata, Regulation of pancreatic beta-cell function by the HNF transcription network: lessons from maturity-onset diabetes of the young (MODY), Endocr. J. 50 (2003) 491–499.
[11] Y. Mineharu, K. Takenaka, H. Yamakawa, K. Inoue, H. Ikeda, K.I. Kikuta, Y. Takagi, K. Nozaki, N. Hashimoto, A. Koizumi, Inheritance pattern of familial moyamoya disease: autosomal dominant mode and genomic imprinting, J. Neurol. Neurosurg. Psychiatry 77 (2006) 1025–1029.
[12] The Committee of Japan Diabetes Society on the diagnostic criteria of diabetes mellitus, Report of the Committee on the classification and diagnostic criteria of diabetes mellitus, J. Jpn Diab. Soc. 53 (2010) 450–467.
[13] L. Kruglyak, M.J. Daly, M.P. Reeve-Daly, E.S. Lander, Parametric and nonparametric linkage analysis: a unified multipoint approach, Am. J. Hum. Genet. 58 (1996) 1347–1363.
[14] S. Aerts, D. Lambrechts, S. Maity, P. Van Loo, B. Coessens, F. De Smet, L.C. Tranchevent, B. De Moor, P. Marynen, B. Hassan, P. Carmeliet, Y. Moreau, Gene prioritization through genomic data fusion, Nat. Biotechnol. 24 (2006) 537–544.
[15] W. Bodmer, C. Bonilla, Common and rare variants in multifactorial susceptibility to common diseases, Nat. Genet. 40 (2008) 695–701.
[16] S. Ellard, C. Bellanne-Chantelot, A.T. Hattersley, Best practice guidelines for the molecular genetic diagnosis of maturity-onset diabetes of the young, Diabetologia 51 (2008) 546–553.
[17] S. Yamada, H. Nishigori, H. Onda, T. Utsugi, T. Yanagawa, T. Maruyama, K. Onigata, K. Nagashima, R. Nagai, A. Morikawa, T. Takeuchi, J. Takeda, Identification of mutations in the hepatocyte nuclear factor (HNF)-1 alpha gene in Japanese subjects with IDDM, Diabetes 46 (1997) 1643–1647.
[18] Q. Zhu, K. Yamagata, A. Miura, N. Shihara, Y. Horikawa, J. Takeda, J. Miyagawa, Y. Matsuzawa, T130I mutation in HNF-4alpha gene is a loss-of-function mutation in hepatocytes and is associated with late-onset Type 2 diabetes mellitus in Japanese subjects, Diabetologia 46 (2003) 567–573.
[19] J. Grimsby, J.W. Coffey, M.T. Dvorozniak, J. Magram, G. Li, F.M. Matschinsky, C. Shiota, S. Kaur, M.A. Magnuson, J.F. Grippo, Characterization of glucokinase regulatory protein-deficient mice, J. Biol. Chem. 275 (2000) 7826–7831.
[20] E.D. Slosberg, U.J. Desai, B. Fanelli, I. St Denny, S. Connelly, M. Kaleko, B.R. Boettcher, S.L. Caplan, Treatment of type 2 diabetes by adenoviral-mediated overexpression of the glucokinase regulatory protein, Diabetes 50 (2001) 1813–1820.
[21] K. Duda, Y.I. Chi, S.E. Shoelson, Structural basis for HNF-4alpha activation by ligand and coactivator binding, J. Biol. Chem. 279 (2004) 23311–23316.
[22] T. Yorifuji, K. Nagashima, K. Kurokawa, M. Kawai, M. Oishi, Y. Akazawa, M. Hosokawa, Y. Yamada, N. Inagaki, T. Nakahata, The C42R mutation in the Kir6.2 (KCNJ11) gene as a cause of transient neonatal diabetes, childhood diabetes, or later-onset, apparently type 2 diabetes mellitus, J. Clin. Endocrinol. Metab. 90 (2005) 3174–3178.
[23] T. Sparso, G. Andersen, T. Nielsen, K.S. Burgdorf, A.P. Gjesing, A.L. Nielsen, A. Albrechtsen, S.S. Rasmussen, T. Jorgensen, K. Borch-Johnsen, A. Sandbaek, T. Lauritzen, S. Madsbad, T. Hansen, O. Pedersen, The GCKR rs780094 polymorphism is associated with elevated fasting serum triacylglycerol, reduced fasting and OGTT-related insulinaemia, and reduced risk of type 2 diabetes, Diabetologia 51 (2008) 70–75.
[24] M. Vaxillaire, C. Cavalcanti-Proenca, A. Dechaume, J. Tichet, M. Marre, B. Balkau, P. Froguel, The common P446L polymorphism in GCKR inversely modulates fasting glucose and triglyceride levels and reduces type 2 diabetes risk in the DESIR prospective general French population, Diabetes 57 (2008) 2253–2257.
[25] M. Orho-Melander, O. Melander, C. Guiducci, P. Perez-Martinez, D. Corella, C. Roos, R. Tewhey, M.J. Rieder, J. Hall, G. Abecasis, E.S. Tai, C. Welch, D.K. Arnett, V. Lyssenko, E. Lindholm, R. Saxena, P.I. de Bakker, N. Burtt, B.F. Voight, J.N. Hirschhorn, K.L. Tucker, T. Hedner, T. Tuomi, B. Isomaa, K.F. Eriksson, M.R. Taskinen, B. Wahlstrand, T.E. Hughes, L.D. Parnell, C.Q. Lai, G. Berglund, L. Peltonen, E. Vartiainen, P. Jousilahti, A.S. Havulinna, V. Salomaa, P. Nilsson, L. Groop, D. Altshuler, J.M. Ordovas, S. Kathiresan, Common missense variant in the glucokinase regulatory protein gene is associated with increased plasma triglyceride and C-reactive protein but lower fasting glucose concentrations, Diabetes 57 (2008) 3112–3121.
[26] Q. Qi, Y. Wu, H. Li, R.J. Loos, F.B. Hu, L. Sun, L. Lu, A. Pan, C. Liu, H. Wu, L. Chen, Z. Yu, X. Lin, Association of GCKR rs780094, alone or in combination with GCK rs1799884, with type 2 diabetes and related traits in a Han Chinese population, Diabetologia 52 (2009) 834–843.
[27] F. Takeuchi, T. Katsuya, S. Chakrewarthy, K. Yamamoto, A. Fujioka, M. Serizawa, T. Fujisawa, E. Nakashima, K. Ohnaka, H. Ikegami, T. Sugiyama, T. Nabika, A. Kasturiratne, S. Yamaguchi, S. Kono, R. Takayanagi, Y. Yamori, S. Kobayashi, T. Ogihara, A. de Silva, R. Wickremasinghe, N. Kato, Common variants at the GCK, GCKR, G6PC2-ABCB11 and MTNR1B loci are associated with fasting glucose in two Asian populations, Diabetologia 53 (2010) 299–308.
[28] R. Saxena, M.F. Hivert, C. Langenberg, T. Tanaka, J.S. Pankow, P. Vollenweider, V. Lyssenko, N. Bouatia-Naji, J. Dupuis, A.U. Jackson, W.H. Kao, M. Li, N.L. Glazer, A.K. Manning, J. Luan, H.M. Stringham, I. Prokopenko, T. Johnson, N. Grarup, T.W. Boesgaard, C. Lecoeur, P. Shrader, J. O'Connell, E. Ingelsson, D.J. Couper, K. Rice, K. Song, C.H. Andreasen, C. Dina, A. Kottgen, O. Le Bacquer, F. Pattou, J. Taneera, V. Steinthorsdottir, D. Rybin, K. Ardlie, M. Sampson, L. Qi, M. van Hoek, M.N. Weedon, Y.S. Aulchenko, B.F. Voight, H. Grallert, B. Balkau, R.N. Bergman, S.J. Bielinski, A. Bonnefond, L.L. Bonnycastle, K. Borch-Johnsen, Y. Bottcher, E. Brunner, T.A. Buchanan, S.J. Bumpstead, C. Cavalcanti-Proenca, G. Charpentier, Y.D. Chen, P.S. Chines, F.S. Collins, M. Cornelis, J.C.G, J. Delplanque, A. Doney, J.M. Egan, M.R. Erdos, M. Firmann, N.G. Forouhi, C.S. Fox, M.O. Goodarzi, J. Graessler, A. Hingorani, B. Isomaa, T. Jorgensen, M. Kivimaki, P. Kovacs, K. Krohn, M. Kumari, T. Lauritzen,

C. Levy-Marchal, V. Mayor, J.B. McAteer, D. Meyre, B.D. Mitchell, K.L. Mohlke, M.A. Morken, N. Narisu, C.N. Palmer, R. Pakyz, L. Pascoe, F. Payne, D. Pearson, W. Rathmann, A. Sandbaek, A.A. Sayer, L.J. Scott, S.J. Sharp, E. Sijbrands, A. Singleton, D.S. Siscovick, N.L. Smith, T. Sparso, A.J. Swift, H. Syddall, G. Thorleifsson, A. Tonjes, T. Tuomi, J. Tuomilehto, T.T. Valle, G. Waeber, A. Walley, D.M. Waterworth, E. Zeggini, J.H. Zhao, T. Illig, H.E. Wichmann, J.F. Wilson, C. van Duijn, F.B. Hu, A.D. Morris, T.M. Frayling, A.T. Hattersley, U. Thorsteinsdottir, K. Stefansson, P. Nilsson, A.C. Syvanen, A.R. Shuldiner, M. Walker, S.R. Bornstein, P. Schwarz, G.H. Williams, D.M. Nathan, J. Kuusisto, M. Laakso, C. Cooper, M. Marmot, L. Ferrucci, V. Mooser, M. Stumvoll, R.J. Loos, D. Altshuler, B.M. Psaty, J.I. Rotter, E. Boerwinkle, T. Hansen, O. Pedersen, J.C. Florez, M.I. McCarthy, M. Boehnke, I. Barroso, R. Sladek, P. Froguel, J.B. Meigs, L. Groop, N.J. Wareham, R.M. Watanabe, Genetic variation in GIPR influences the glucose and insulin responses to an oral glucose challenge, Nat. Genet. 42 (2010) 142–148.

[29] J. Dupuis, C. Langenberg, I. Prokopenko, R. Saxena, N. Soranzo, A.U. Jackson, E. Wheeler, N.L. Glazer, N. Bouatia-Naji, A.L. Gloyn, C.M. Lindgren, R. Magi, A.P. Morris, J. Randall, T. Johnson, P. Elliott, D. Rybin, G. Thorleifsson, V. Steinthorsdottir, P. Henneman, H. Grallert, A. Dehghan, J.J. Hottenga, C.S. Franklin, P. Navarro, K. Song, A. Goel, J.R. Perry, J.M. Egan, T. Lajunen, N. Grarup, T. Sparso, A. Doney, B.F. Voight, H.M. Stringham, M. Li, S. Kanoni, P. Shrader, C. Cavalcanti-Proenca, M. Kumari, L. Qi, N.J. Timpson, C. Gieger, C. Zabena, G. Rocheleau, E. Ingelsson, P. An, J. O'Connell, J. Luan, A. Elliott, S.A. McCarroll, F. Payne, R.M. Roccasecca, F. Pattou, P. Sethupathy, K. Ardlie, Y. Ariyurek, B. Balkau, P. Barter, J.P. Beilby, Y. Ben-Shlomo, R. Benediktsson, A.J. Bennett, S. Bergmann, M. Bochud, E. Boerwinkle, A. Bonnefond, L.L. Bonnycastle, K. Borch-Johnsen, Y. Bottcher, E. Brunner, S.J. Bumpstead, G. Charpentier, Y.D. Chen, P. Chines, R. Clarke, L.J. Coin, M. N. Cooper, M. Cornelis, G. Crawford, L. Crisponi, I.N. Day, E.J. de Geus, J. Delplanque, C. Dina, M.R. Erdos, A.C. Fedson, A. Fischer-Rosinsky, N.G. Forouhi, C.S. Fox, R. Frants, M.G. Franzosi, P. Galan, M.O. Goodarzi, J. Graessler, C.J. Groves, S. Grundy, R. Gwilliam, U. Gyllensten, S. Hadjadj, G. Hallmans, N. Hammond, X. Han, A.L. Hartikainen, N. Hassanali, C. Hayward, S.C. Heath, S. Hercberg, C. Herder, A.A. Hicks, D.R. Hillman, A.D. Hingorani, A. Hofman, J. Hui, J. Hung, B. Isomaa, P.R. Johnson, T. Jorgensen, A. Jula, M. Kaakinen, J. Kaprio, Y.A. Kesaniemi, M. Kivimaki, B. Knight, S. Koskinen, P. Kovacs, K.O. Kyvik, G.M. Lathrop, D.A. Lawlor, O. Le Bacquer, C. Lecoeur, Y. Li, V. Lyssenko, R. Mahley, M. Mangino, A.K. Manning, M.T. Martinez-Larrad, J.B. McAteer, L.J. McCulloch, R. McPherson, C. Meisinger, D. Melzer, D. Meyre, B.D. Mitchell, M.A. Morken, S. Mukherjee, S. Naitza, N. Narisu, M. J. Neville, B.A. Oostra, M. Orru, R. Pakyz, C.N. Palmer, G. Paolisso, C. Pattaro, D. Pearson, J.F. Peden, N.L. Pedersen, M. Perola, A.F. Pfeiffer, I. Pichler, O. Polasek, D. Posthuma, S.C. Potter, A. Pouta, M.A. Province, B.M. Psaty, W. Rathmann, N.W. Rayner, K. Rice, S. Ripatti, F. Rivadeneira, M. Roden, O. Rolandsson, A. Sandbaek, M. Sandhu, S. Sanna, A.A. Sayer, P. Scheet, L.J. Scott, U. Seedorf, S.J. Sharp, B. Shields, G. Sigurethsson, E.J. Sijbrands, A. Silveira, L. Simpson, A. Singleton, N.L. Smith, U. Sovio, A. Swift, H. Syddall, A.C. Syvanen, T. Tanaka, B. Thorand, J. Tichet, A. Tonjes, T. Tuomi, A.G. Uitterlinden, K.W. van Dijk, M. van Hoek, D. Varma, S. Visvikis-Siest, V. Vitart, N. Vogelzangs, G. Waeber, P.J. Wagner, A. Walley, G.B. Walters, K.L. Ward, H. Watkins, M.N. Weedon, S.H. Wild, G. Willemsen, J.C. Witteman, J.W. Yarnell, E. Zeggini, D. Zelenika, B. Zethelius, G. Zhai, J.H. Zhao, M.C. Zillikens, I.B. Borecki, R.J. Loos, P. Meneton, P.K. Magnusson, D.M. Nathan, G.H. Williams, A.T. Hattersley, K. Silander, V. Salomaa, G.D. Smith, S.R. Bornstein, P. Schwarz, J. Spranger, F. Karpe, A. R. Shuldiner, C. Cooper, G.V. Dedoussis, M. Serrano-Rios, A.D. Morris, L. Lind, L.J. Palmer, F.B. Hu, P.W. Franks, S. Ebrahim, M. Marmot, W.H. Kao, J.S. Pankow, M.J. Sampson, J. Kuusisto, M. Laakso, T. Hansen, O. Pedersen, P.P. Pramstaller, H.E. Wichmann, T. Illig, I. Rudan, A.F. Wright, M. Stumvoll, H. Campbell, J.F. Wilson, R.N. Bergman, T.A. Buchanan, F.S. Collins, K.L. Mohlke, J. Tuomilehto, T.T. Valle, D. Altshuler, J.I. Rotter, D.S. Siscovick, B.W. Penninx, D.I. Boomsma, P. Deloukas, T.D. Spector, T.M. Frayling, L. Ferrucci, A. Kong, U. Thorsteinsdottir, K. Stefansson, C.M. van Duijn, Y.S. Aulchenko, A. Cao, A. Scuteri, D. Schlessinger, M. Uda, A. Ruokonen, M.R. Jarvelin, D.M. Waterworth, P. Vollenweider, L. Peltonen, V. Mooser, G.R. Abecasis, N.J. Wareham, R. Sladek, P. Froguel, R.M. Watanabe, J.B. Meigs, L. Groop, M. Boehnke, M.I. McCarthy, J.C. Florez, I. Barroso, New genetic loci implicated in fasting glucose homeostasis and their impact on type 2 diabetes risk, Nat. Genet. 42 (2010) 105–116.

[30] H. Onuma, Y. Tabara, R. Kawamoto, I. Shimizu, R. Kawamura, Y. Takata, W. Nishida, J. Ohashi, T. Miki, K. Kohara, H. Makino, H. Osawa, The GCKR rs780094 polymorphism is associated with susceptibility of type 2 diabetes, reduced fasting plasma glucose levels, increased triglycerides levels and lower HOMA-IR in Japanese population, J. Hum. Genet. 55 (2010) 600–604.

[31] C.T. Johansen, J. Wang, M.B. Lanktree, H. Cao, A.D. McIntyre, M.R. Ban, R.A. Martins, B.A. Kennedy, R.G. Hassell, M.E. Visser, S.M. Schwartz, B.F. Voight, R. Elosua, V. Salomaa, C.J. O'Donnell, G.M. Dallinga-Thie, S.S. Anand, S. Yusuf, M.W. Huff, S. Kathiresan, R.A. Hegele, Excess of rare variants in genes identified by genome-wide association study of hypertriglyceridemia, Nat. Genet. 42 (2010) 684–687.

[32] B.E. Hayward, N. Dunlop, S. Intody, J.P. Leek, A.F. Markham, J.P. Warner, D.T. Bonthron, Organization of the human glucokinase regulator gene GCKR, Genomics 49 (1998) 137–142.

[33] D.D. Licatalosi, R.B. Darnell, RNA processing and its regulation: global insights into biological networks, Nat. Rev. Genet. 11 (2010) 75–87.

[34] T. Heinemeyer, E. Wingender, I. Reuter, H. Hermjakob, A.E. Kel, O.V. Kel, E.V. Ignatieva, E.A. Ananko, O.A. Podkolodnaya, F.A. Kolpakov, N.L. Podkolodny, N.A. Kolchanov, Databases on transcriptional regulation: TRANSFAC, TRRD, and COMPEL, Nucleic Acids Res. 26 (1998) 364–370.

Biochemical and Biophysical Research Communications 404 (2011) 115–120

Contents lists available at ScienceDirect

Biochemical and Biophysical Research Communications

journal homepage: www.elsevier.com/locate/ybbrc

# The effect of gastric inhibitory polypeptide on intestinal glucose absorption and intestinal motility in mice

Eiichi Ogawa [a], Masaya Hosokawa [a,b], Norio Harada [a], Shunsuke Yamane [a], Akihiro Hamasaki [a], Kentaro Toyoda [a], Shimpei Fujimoto [a], Yoshihito Fujita [a], Kazuhito Fukuda [a], Katsushi Tsukiyama [a,c], Yuichiro Yamada [a,c], Yutaka Seino [a,d], Nobuya Inagaki [a,e,*]

[a] Department of Diabetes and Clinical Nutrition, Graduate School of Medicine, Kyoto University, Japan
[b] Faculty of Human Sciences, Tezukayama Gakuin University, Osaka, Japan
[c] Department of Internal Medicine, Division of Endocrinology, Diabetes and Geriatric Medicine, Akita University School of Medicine, Akita, Japan
[d] Kansai Electric Power Hospital, Osaka, Japan
[e] CREST of Japan Science and Technology Cooperation (JST), Kyoto, Japan

ARTICLE INFO

*Article history:*
Received 21 October 2010
Available online 21 November 2010

*Keywords:*
GIP
Glucose absorption
Intestine

ABSTRACT

Gastric inhibitory polypeptide (GIP) is released from the small intestine upon meal ingestion and increases insulin secretion from pancreatic β cells. Although the GIP receptor is known to be expressed in small intestine, the effects of GIP in small intestine are not fully understood. This study was designed to clarify the effect of GIP on intestinal glucose absorption and intestinal motility. Intestinal glucose absorption *in vivo* was measured by single-pass perfusion method. Incorporation of [$^{14}$C]-glucose into everted jejunal rings *in vitro* was used to evaluate the effect of GIP on sodium-glucose co-transporter (SGLT). Motility of small intestine was measured by intestinal transit after oral administration of a non-absorbed marker. Intraperitoneal administration of GIP inhibited glucose absorption in wild-type mice in a concentration-dependent manner, showing maximum decrease at the dosage of 50 nmol/kg body weight. In glucagon-like-peptide-1 (GLP-1) receptor-deficient mice, GIP inhibited glucose absorption as in wild-type mice. *In vitro* examination of [$^{14}$C]-glucose uptake revealed that 100 nM GIP did not change SGLT-dependent glucose uptake in wild-type mice. After intraperitoneal administration of GIP (50 nmol/kg body weight), small intestinal transit was inhibited to 40% in both wild-type and GLP-1 receptor-deficient mice. Furthermore, a somatostatin receptor antagonist, cyclosomatostatin, reduced the inhibitory effect of GIP on both intestinal transit and glucose absorption in wild-type mice. These results demonstrate that exogenous GIP inhibits intestinal glucose absorption by reducing intestinal motility through a somatostatin-mediated pathway rather than through a GLP-1-mediated pathway.



## 1. Introduction

Gastric inhibitory polypeptide (GIP), also called glucose-dependent insulinotropic polypeptide, is an incretin of 42-amino-acid polypeptide synthesized by K cells of the duodenum and small intestine [1]. We previously generated GIP receptor-deficient mice (GIPR$^{-/-}$ mice) and showed that GIPR$^{-/-}$ mice have higher blood glucose levels as well as impaired initial insulin response after oral glucose load [2]. Thus, early insulin secretion stimulated by GIP plays an important role in glucose tolerance after oral glucose load.

While GIP receptor mRNA was reported to be present in rat gut [3], the role of the GIP receptor in the gut has not been fully clarified. In this *in vivo* study, we investigated the effect of exogenous GIP on intestinal glucose absorption in mice using the intestinal perfusion method. We investigated the effect of exogenous GIP on SGLT-dependent glucose uptake *in vitro* by using the everted jejunal ring method. Because intestinal motility and absorption are positively related [4,5], we investigated the effect of exogenous GIP on gastrointestinal motility by non-absorbed marker method. Since SST secretion has been reported to be stimulated by GIP and to prolong intestinal motility, we also investigated the involvement of SST in the inhibitory effect of exogenous GIP on both intestinal transit and intestinal glucose absorption by using somatostatin receptor antagonist. Our results demonstrate that exogenous GIP inhibits intestinal glucose absorption by reducing intestinal motility through a somatostatin-mediated pathway rather than through a GLP-1-mediated pathway.

*Abbreviations:* GIP, Gastric inhibitory polypeptide; GLP-1, glucagon-like-peptide-1; SST, somatostatin; SGLT, sodium-glucose co-transporter; CSS, cyclosomatostatin.

* Corresponding author. Address: Department of Diabetes and Clinical Nutrition, Graduate School of Medicine, Kyoto University, 54 Shogoin, Kawahara-cho, Sakyo-ku, Kyoto 606-8507, Japan. Fax: +81 75 771 6601.
*E-mail address:* inagaki@metab.kuhp.kyoto-u.ac.jp (N. Inagaki).

0006-291X/$ - see front matter © 2010 Elsevier Inc. All rights reserved.
doi:10.1016/j.bbrc.2010.11.077